Centrality determination in MPD experiment using multiplicity of produced charged particles

Petr Parfenov, Dim Idrisov, Vinh Ba Luong, Arkadiy Taranenko
(for the MPD Collaboration)

NRNU MEPhI, Moscow, Russia

Analysis Note draft
March 2021

1 Introduction

The size and evolution of the medium created in a heavy-ion collision depends on collision geometry which is defined by the geometric parameters such as impact parameter vector, number of participants and binary collisions. Those parameters cannot be measured directly. Experimentally, collisions are characterized by the measured particle multiplicities around midrapidity, or by the energy measured in the forward rapidity region, which is sensitive to the spectator fragments. For centrality definition based on the charged particle multiplicity, collisions are grouped into centrality classes with the most central class defined by events with the highest multiplicity which corresponds to small values of the impact parameter and vice versa:

$$c_{N_{ch}} = \frac{1}{\sigma_{inel}} \int_{N_{ch}}^{\infty} \frac{d\sigma}{dN_{ch}} dN_{ch}, \tag{1}$$

where σ_{inel} is the inelastic cross-section of a nucleus-nucleus collision, $\frac{d\sigma}{dN_{ch}}$ – is the probability that inelastic collision occurs at given multiplicity N_{ch}. Usually the total inelastic cross-section is substituted with a total number of collisions corrected for a trigger inefficiency and bias. In this method, Glauber Monte Carlo (MC-Glauber) is used to do this correction.

1.1 Centrality determination in the experiments

In the experiments, one of the methods for centrality determination is Glauber Monte Carlo based method using multiplicity distribution in midrapidity range. It is widely used in the existing experiments such as ALICE (LHC) [1], NA49 (SPS) [2], STAR (BNL) [3] and future experiment CBM (SIS-100) [4].

Besides that, overall procedure is similar to the one discussed below: fit function for multiplicity distribution is build based on Glauber Monte Carlo calculations, centrality classes are defined by sharp cuts on multiplicity distribution, and resulting geometric parameters such as impact parameter b, number of participant nuclei N_{part} and binary nucleon-nucleon collisions N_{coll} for each centrality classes are taken from Glauber Monte Carlo calculations. Figure 1 shows the uncorrected multiplicity

$N_{\rm ch}^{\rm raw}$ distribution for charged particles from the data at $\sqrt{s_{NN}}$ = 7.7, 11.5, 19.6, 27 and 39 GeV compared to those from Monte Carlo (MC) Glauber fit. The figure is taken from ref. [3]. The fit function here was defined using two-component model [3], [5]:

$$\frac{1}{N}\frac{dN}{dN_{ch}} = n_{pp}\left[(1-x)\frac{N_{part}}{2} + xN_{coll}\right], \tag{2}$$

where n_{pp} is the average multiplicity per unit of pseudorapidity in minimum-bias p+p collisions and x – is the fraction of production from the hard component which acts here as a fit parameter.

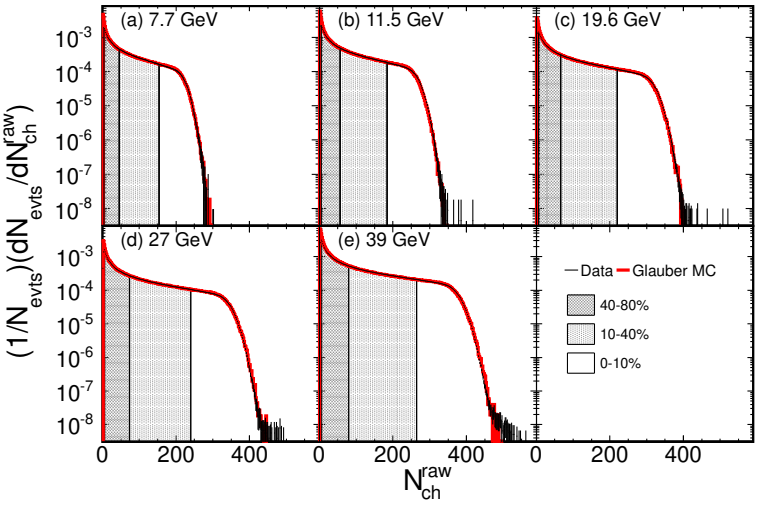

Figure 1: Distribution of uncorrected multiplicity $N_{\rm ch}^{\rm raw}$ measured in STAR experiment within $|\eta| < 0.5$ in the TPC from $\sqrt{s_{NN}}$ = 7.7 to 39 GeV in Au + Au collisions shown as black points. The red curves show the multiplicity distributions at $\sqrt{s_{NN}}$ = 7.7 to 39 GeV from MC Glauber simulations [3].

2 The Glauber Monte Carlo

2.1 Nuclear charge distribution

Glauber Monte Carlo provides a simple tool to to describe the initial state distribution of nucleons in heavy-ion collisions [6].

A collision is described as set of individual interactions of the constituent nucleons. It is assumed that nucleons move independently inside the nucleus and pass each other without deflection during collision. Size of the nucleus is considered to be large compared to the range of nucleon-nucleon force. The nucleon density inside the nucleus is provided as an input of the Glauber model. This density can be described by the Fermi (or modified Woods-Saxon) distribution:

$$\rho(r) = \rho_0 \frac{1 + w\left(\frac{r}{R}\right)^2}{1 + \exp\frac{r-R}{a}}, \tag{3}$$

where R is radius of the nucleus, ρ_0 is density in the center of the nucleus, a is the skin thickness of the nucleus which defines how quickly the nuclear density falls off near the edge of the nucleus. The additional parameter w is needed to describe nuclei whose maximum density is reached at radii $r > 0$. For ^{197}Au and ^{209}Bi those parameters are listed in the table 1 [7], [8].

	R, fm	a, fm	w
^{197}Au	6.5541	0.544	0
^{209}Bi	6.75	0.468	0

Table 1: Parameters of the Fermi (or modified Woods-Saxon) distribution for ^{197}Au and ^{209}Bi.

2.2 Inelastic nucleon-nucleon cross-section

The second step is to simulate a nuclear collision. The nucleus-nucleus collision is treated as a sequence of independent binary nucleon-nucleon collisions, where the nucleons travel on straight-line trajectories and the inelastic nucleon-nucleon cross section is assumed to be independent of the number of collisions a nucleon underwent previously, i.e. the same cross section is used for all successive collisions. Two nucleons from different nuclei are assumed to collide if the relative transverse distance between centers is less than the distance corresponding to the inelastic nucleon-nucleon cross section σ_{NN}^{inel}:

$$d < \sqrt{\frac{\sigma_{NN}^{inel}}{\pi}}. \tag{4}$$

The inelastic nucleon-nucleon cross sections used here is based on total cross section measurements for p+p collisions ($\pm$1 mb uncertainty) and elastic total cross sections for p+p and p+$\bar{\text{p}}$ ($\pm$0.5 mb error) [9]. Values of σ_{NN}^{inel} for energies corresponding to the NICA range are listed in the table 2 [10].

$\sqrt{s_{NN}}$, GeV	4.5	7.7	9.5	11
σ_{NN}^{inel}, mb	29.3	29.7	30.8	31.2

Table 2: The inelastic nucleon-nucleon cross sections for energies corresponding to the NICA energy range.

2.3 The NBD Glauber fit to the multiplicity distribution

This work follows the Centrality determination framework implementation in CBM experiment [4] developed by Viktor Klochkov and Ilya Selyuzhenkov. To reproduce the experimental multiplicity distribution and to estimate the trigger bias, the MC-Glauber is coupled to a model for particle production, based on a negative binomial distribution (NBD) $P_{\mu,k}(N_{ch})$ which describes charged particle multiplicity $d\sigma/dN_{ch}$ for p+p collisions:

$$P_{\mu,k}(n) = \frac{\Gamma(n+k)}{\Gamma(n+1)\Gamma(k)} \cdot \frac{(\mu/k)^n}{(\mu/k+1)^{n+k}}. \tag{5}$$

In the case of A+A collisions we introduce the concept of "ancestors" N_a – set of independently emitting sources of particles. N_a depends on number of participant nucleons N_{part} and number of

binary nucleon-nucleon collisions N_{coll} provided by the Glauber model and it can be parametrized in several ways:

- "Default": $N_a(f) = fN_{part} + (1-f)N_{coll}$,
- "PSD": $N_a(f) = f - N_{part}$,
- "Npart": $N_a(f) = (N_{part})^f$,
- "Ncoll": $N_a(f) = (N_{coll})^f$,
- "STAR": $N_a(f) = \frac{(1-f)}{2}N_{part} + fN_{coll}$.

The "Default" parametrization is set as a main one and the others are used during systematic check. Resulting Glauber-based fit function for the experimentally measured charged particle multiplicity can be defined as following:

$$\frac{d\sigma}{dN_{ch}} \equiv F_{fit}(f,\mu,k) = N_a(f) \times P_{\mu,k}(N_{ch}). \tag{6}$$

This fit function has 3 parameters: f, k and μ. The first parameter f defines the fit function shape and can be connected with the type of nucleon-nucleon interaction. The second parameter μ is the mean number of tracks in the detector produced by one source (ancestor). The last parameter k defines the spread in multiplicities for a given set of emmiting sources N_a and can be connected to fluctuations.
A minimization procedure is applied to find the optimal set of parameters which result in the smallest fitting criteria $\chi^2_{measured}$ defined as follows:

$$\chi^2_{measured} = \sum_{i=n_{low}}^{n_{high}} \frac{\left(F^i_{fit} - F^i_{data}\right)^2}{\left(\Delta F^i_{fit}\right)^2 + \left(\Delta F^i_{data}\right)^2}, \tag{7}$$

where F^i_{fit} and F^i_{data} are values of the fit function and fitted histogram at a given bin i, ΔF^i_{fit} and ΔF^i_{data} are corresponding uncertainties, n_{low} and n_{high} are the lowest and highest fitting ranges correspondingly. The value $\chi^2_{measured}$ is then divided over the number of fitted bins representing the number of degrees of freedom:

$$\chi^2 = \frac{\chi^2_{measured}}{n_{high} - n_{low}}. \tag{8}$$

The best fit has $\chi^2 \to 1$.
At some point, the contributions from the trigger and from the electromagnetic interactions bias the measured distribution. At this point, the data and the fit start to diverge. Below this point, which is called the "anchor" point, the centrality determination is not reliable.
With the MC-Glauber fit one has the connection between measured collisions and simulated collisions with the Glauber model. One can then calculate the mean values of impact parameter $\langle b \rangle$, number of participants $\langle N_{part} \rangle$ and NN binary collisions $\langle N_{coll} \rangle$ for centrality classes defined by sharp cuts in the charged particle multiplicity.

3 The Bayesian inversion method

This method for centrality determination was suggested by Rudolph Rogly, Giuliano Giacalone and Jean-Yves Ollitrault [11], [12]. The Bayesian inversion method (Γ-fit) allows to reconstruct impact parameter distribution from charge particle multiplicity without relying on any specific model of the collision dynamics, such as the Glauber model. The relationship between the experimentally observable multiplicity of produced charged particles N_{ch} and impact parameter b of the colliding nuclei is defined by the probability distribution $P(N_{ch}|b)$ of the charge particle multiplicity N_{ch} for the fixed impact parameter b [11]:

$$P(N_{ch}|b) = \frac{1}{\Gamma(k)\theta^k} N_{ch}^{k-1} e^{-N_{ch}/\theta} \tag{9}$$

where $\Gamma(k) \equiv \int_0^\infty x^{k-1}e^{-x}dx$ is gamma function, k and θ are two positive parameters, which generally depend on b. Parameters k and θ define the shape of the multiplicity distribution and can be attributed to the mean $\langle N_{ch}\rangle$ and standard deviation $\sigma_{N_{ch}}$ of the multiplicity distribution:

$$\langle N_{ch}\rangle = k\theta,\ \sigma_{N_{ch}} = \sqrt{k}\theta. \tag{10}$$

The experimental distribution of produced charged particles can be parametrized using $P(N_{ch}|b)$ over all impact parameters:

$$\frac{1}{M} M_{\Gamma-fit} \equiv P(N_{ch}) = \int_0^\infty P(N_{ch}|b)P(b)db,\ P(b) = \frac{2\pi b}{\sigma_{inel}} P_{inel}(b). \tag{11}$$

Here $1/M$ denotes that the distribution is normalized $\int P(N_{ch})dN_{ch} = 1$. $P_{inel}(b)$ – is the probability for an inelastic collision to occur at given b, and σ_{inel} – is the inelastic nucleus-nucleus cross section. The inelastic cross section can be obtained as a result of fitting the probability distribution of impact parameter (fig. 2) by the linear function as well as calculated from the Glauber Monte Carlo model for Au+Au and Bi+Bi collisions at $\sqrt{s_{NN}} = 7.7$ GeV. We find σ_{inel} =677 fm^2 in Au+Au collisions, and σ_{inel} = 687 fm^2 in Bi+Bi collisions. For non-peripheral collisions we can assume that the probability for an inelastic collision close to 1 ($P(b) \approx \frac{2\pi b}{\sigma_{inel}}$). Following the ref. [11], we change variables from b to its cumulative probability distribution c_b:

$$c_b = \int_0^b P(b')db'. \tag{12}$$

The left side of equation (11) then is simplified to

$$P(N_{ch}) = \int_0^1 P(N_{ch}|c_b)dc_b. \tag{13}$$

where $P(N_{ch}|c_b)$ denotes the probability distribution of N_{ch} at fixed c_b, i.e., fixed b. To define the variable k we used the following parameterization:

$$k(b) = k_0 \cdot exp\left[-\sum_{i=1}^{3} a_i \left(c_b\right)^i\right], \tag{14}$$

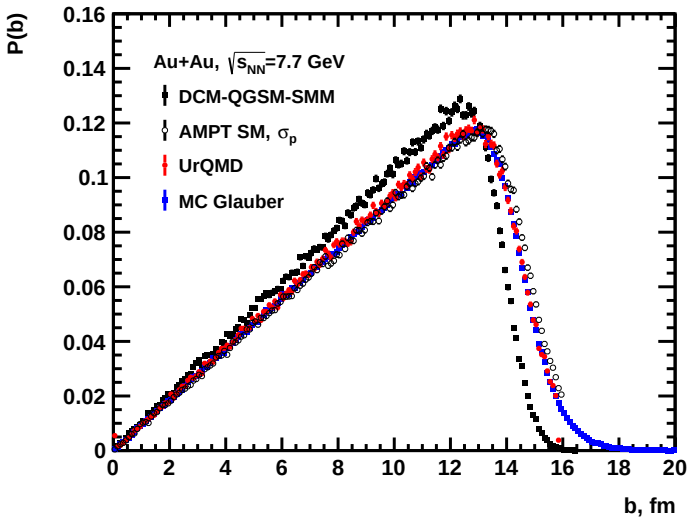

Figure 2: Probability distribution of impact parameter for Au+Au collisions at $\sqrt{s_{NN}}$= 7.7 GeV extracted from different models. Black circle: DCM-QGMS-SMM model. Open circle: AMPT SM $\sigma_p = 1.5mb$. Red circle: UrQMD and blue circle: MC Glauber.

As a result, we have five fitting parameters θ, k_0 and a_i. In this work we use $N_{knee} \equiv k_0\theta$ instead of k_0 for convenience. An example of charged particle multiplicity distribution from UrQMD model (open squares) with Γ-fit function (red circles) is shown on the fig. 3.

Once the set of parameters k_0, a_i and θ is found, the probability distribution $P(b|N_{ch})$ of impact parameter b for fixed centrality classes defined by sharp multiplicity cuts N_{ch}^{low} and N_{ch}^{high} can be introduced using Bayes' theorem:

$$P(b|N_{ch}^{low} < N_{ch} < N_{ch}^{high}) = P(b)\frac{\int\limits_{N_{ch}^{low}}^{N_{ch}^{high}} P(N'_{ch}|b)dN'_{ch}}{\int\limits_{N_{ch}^{low}}^{N_{ch}^{high}} P(N'_{ch})dN'_{ch}}. \quad (15)$$

Using the resulting probability distribution $P(b|N_{ch})$ we can calculate centrality classes and corresponding mean values of impact parameter .

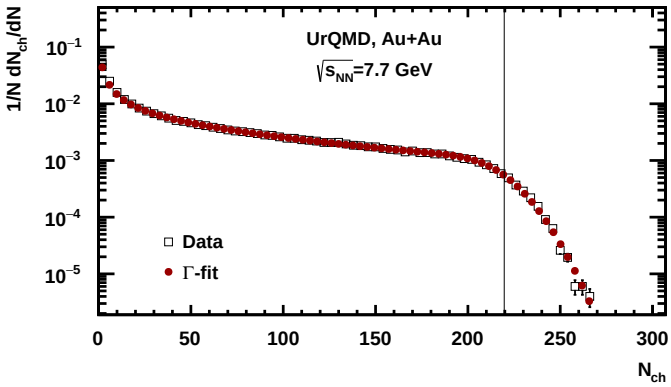

Figure 3: Charged particle multiplicity distribution from the UrQMD model (open squares) for Au+Au collisions at $\sqrt{s_{NN}}$ =7.7 GeV compared to the fitted distribution using Γ-fit approach (red circles).

4 Results

Several models were used in this work: UrQMD [13], AMPT [14], DCMQGSM-SMM [15], [16] and PHQMD [17]. Study was done using model data from UrQMD (version 3.4) in the cascade mode, AMPT (version v1.26t9b-v2.26t9b) in string melting (SM) mode with the value of partonic cross section $\sigma_p = 1.5$ mb, and DCM-QGSM-SMM models. Results for those models are given in section 4.1. Fully reconstructed data with simulated detector responce via GEANT4 also was used. UrQMD and PHQMD were used there as event generators. Results for reconstructed data are given in sections 4.2 and 4.3.

Multiplicity distributions were collected using the same statistics $N_{events} = 5 \cdot 10^5$ and selection criteria for particles/tracks:

- $p_T > 0.15$ GeV/c;
- $|\eta| < 0.5$;
- Only charged particles (for pure models);
- Primary track selection: |DCA| < 0.5 cm (for reconstructed data);
- $N_{ch} > 16$ (for reconstructed data).

To produce the fit functions of multiplicity distributions in Glauber-based method, initial parameters were taken in the following ranges:

- $0 < f < 1$ (for $N_a = N_{part}^f$ parametrization $1 < f < 2$ was used);
- $0 < k < 100$;
- Fit ranges: $N_{ch} > 10$ for $\sqrt{s_{NN}} = 4.5$ GeV and reconstructed data, $N_{ch} > 20$ for $\sqrt{s_{NN}} > 4.5$ GeV.

In the following sections all tables share the similar layout. It is briefly explained here for more readability:

- Centrality – given centrality class (in percents);
- N_{ch}^{min}, N_{ch}^{max} – cuts on the multiplicity distribution for given centrality class $N_{ch}^{min} < N_{ch} < N_{ch}^{max}$;
- $\langle b \rangle$ – mean value of impact parameter b for given centrality class with its RMS value;
- b_{min}, b_{max} – lower and higher estimations of $\langle b \rangle$ for given centrality class obtained from polynomial fit of $\langle b \rangle$ centrality dependence;
- $\langle N_{part} \rangle$ – mean value of number of participant nucleons for given centrality class with its RMS value;
- N_{part}^{min}, N_{part}^{max} – lower and higher estimations of $\langle N_{part} \rangle$ for given centrality class obtained from polynomial fit of $\langle N_{part} \rangle$ centrality dependence;
- $\langle N_{coll} \rangle$ – mean value of number of binary nucleon-nucleon collisions for given centrality class with its RMS value;
- N_{coll}^{min}, N_{coll}^{max} – lower and higher estimations of $\langle N_{coll} \rangle$ for given centrality class obtained from polynomial fit of $\langle N_{coll} \rangle$ centrality dependence.

4.1 Au+Au collisions for $\sqrt{s_{NN}}$=4.5, 7.7 and 11.5 GeV from UrQMD, AMPT and DCM-QGSM-SMM models

Figures 4-9 show charged particle distribution for Au+Au collisions at $\sqrt{s_{NN}} = 4.5$, 7.7 and 11.5 GeV from UrQMD, AMPT SM σ_p=1.5 mb and DCM-QGSM-SMM models correspondingly.

The results of the fitting procedure are shown by blue triangles for CM-Gl and by red circles for Γ-fit approaches.

Figures 10-13 show centrality dependence of mean values of impact parameter $\langle b \rangle$, number of participants $\langle N_{part} \rangle$ and NN binary collisions $\langle N_{coll} \rangle$ for Au+Au collisions at $\sqrt{s_{NN}}$=4.5, 7.7 and 11.5 GeV from UrQMD model.

Figures 14-17 and figs. 18-21 show the same set of figures for AMPT model in the SM mode with partonic cross section σ_p=1.5 mb and DCM-QGMS-SMM model correspondingly.

The parameters of the Γ-fit for Au+Au collisions at $\sqrt{s_{NN}}$ =4.5, 7.7 and 11.5 GeV and the lower bound of multiplicity of the fitting area can be seen in the tables 3-11. Fit parameters for Glauber-based method are listed in the corresponding plots.

Tables 12-14 show geometric properties (b, N_{part}, N_{coll}) of Au+Au collisions at $\sqrt{s_{NN}} = 4.5$ GeV from UrQMD, AMPT SM with σ_p=1.5 mb and DCM-QGSM-SMM models for centrality classes defined by sharp cuts in the charged particle multiplicity distribution, simulated with an NBD-Glauber fit. The mean values and the RMS are obtained with a Glauber Monte Carlo calculation.

Tables 15-17 and tables 18-20 show similar set of geometric properties (b, N_{part}, N_{coll}) for $\sqrt{s_{NN}}$ = 7.7 and 11.5 GeV correspondingly.

Tables 21-23 show geometric properties obtained with a Γ-fit calculation for Au+Au collisions at $\sqrt{s_{NN}} = 4.5$ GeV from UrQMD, AMPT SM with σ_p=1.5 mb and DCM-QGSM-SMM models.

Tables 24-29 show similar set of geometric properties obtained with a Γ-fit calculation for $\sqrt{s_{NN}}$ = 7.7 and 11.5 GeV correspondingly.

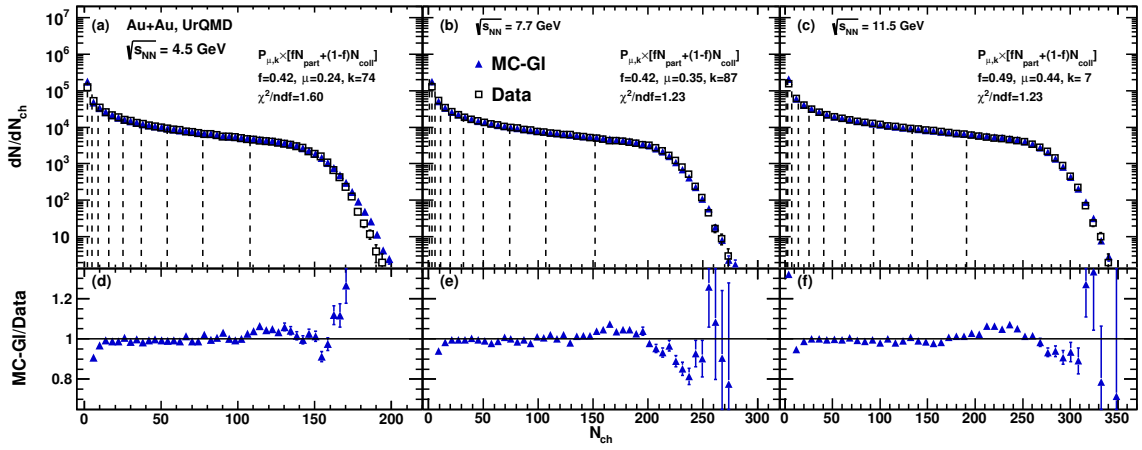

Figure 4: Distribution of the charged particle multiplicity for Au+Au collisions at at $\sqrt{s_{NN}}$=4.5, 7.7 and 11.5 GeV from UrQMD model (open symbols). The distribution is fitted with the Glauber-based fit function (closed symbols). Vertical lines denote sharp cuts for centrality classes.

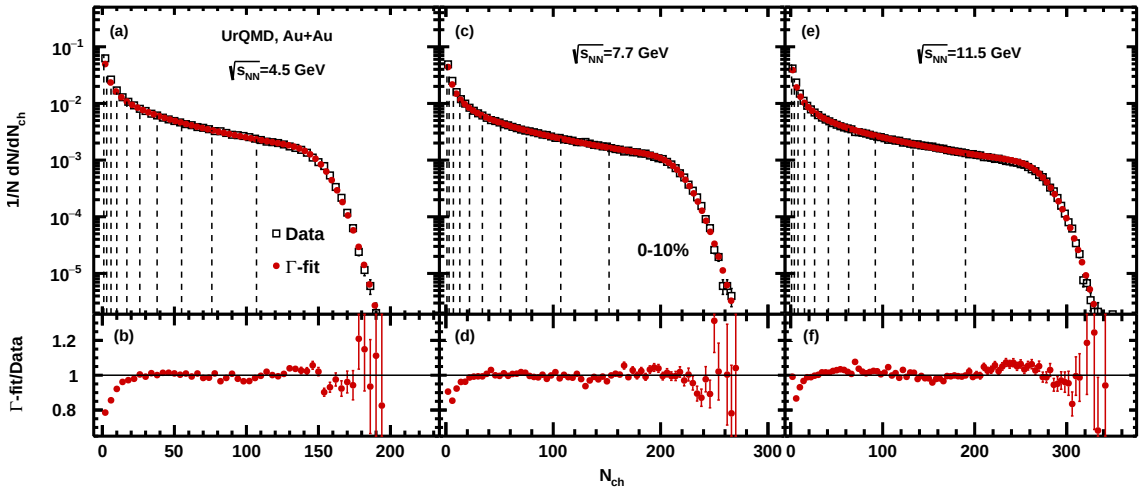

Figure 5: Charged particle multiplicity distribution from the UrQMD model (open squares) for Au+Au collisions at $\sqrt{s_{NN}}$ =4.5, 7.7 and 11.5 GeV compared to the fitted distribution using Γ-fit (red circles) approach. Bottom plots show ratio of the resulted fit functions to the charged particle multiplicity distribution.

θ	N_{knee}	a_1	a_2	a_3	χ^2	NDF	$N_{ch}^{fit}(min)$
0.91	152.82	-4.33	2.46	-4.54	226.27	169.00	20

Table 3: Parameters of the fit to the charged particle multiplicity of the UrQMD model for Au+Au collisions at $\sqrt{s_{NN}}$ =4.5 GeV.

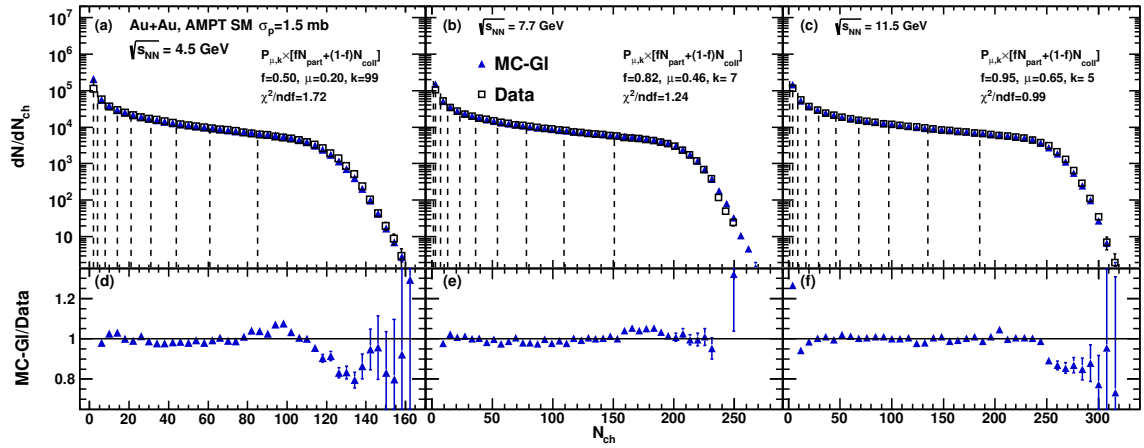

Figure 6: Distribution of the charged particle multiplicity for Au+Au collisions at at $\sqrt{s_{NN}}$=4.5, 7.7 and 11.5 GeV from AMPT SM model with σ_p=1.5 mb model (open symbols). The distribution is fitted with the Glauber-based fit function (closed symbols). Vertical lines denote sharp cuts for centrality classes.

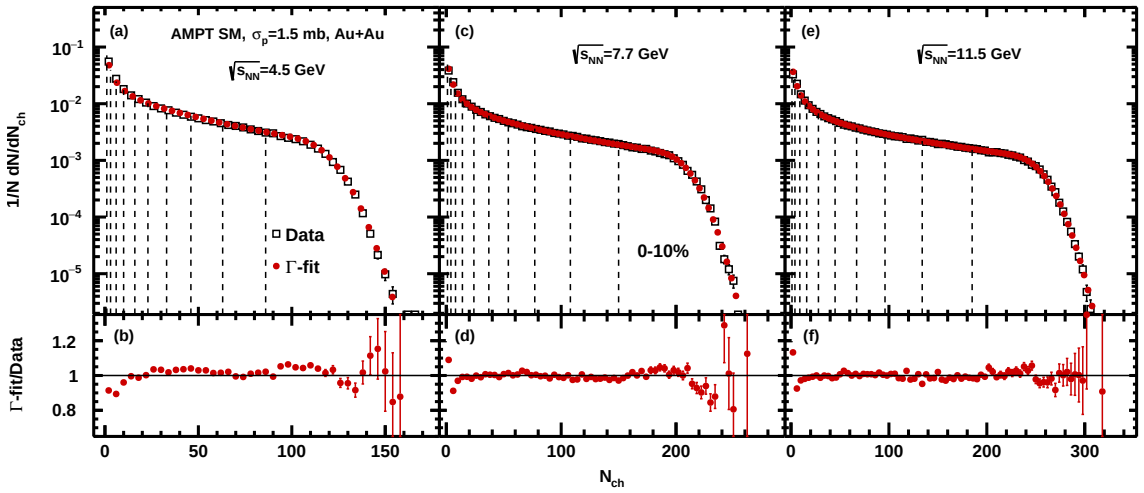

Figure 7: Charged particle multiplicity distribution from the AMPT model (open squares) for Au+Au collisions at $\sqrt{s_{NN}}$ =4.5, 7.7 and 11.5 GeV compared to the fitted distribution using Γ-fit (red circles) approach. Bottom plots show ratio of the resulted fit functions to the charged particle multiplicity distribution.

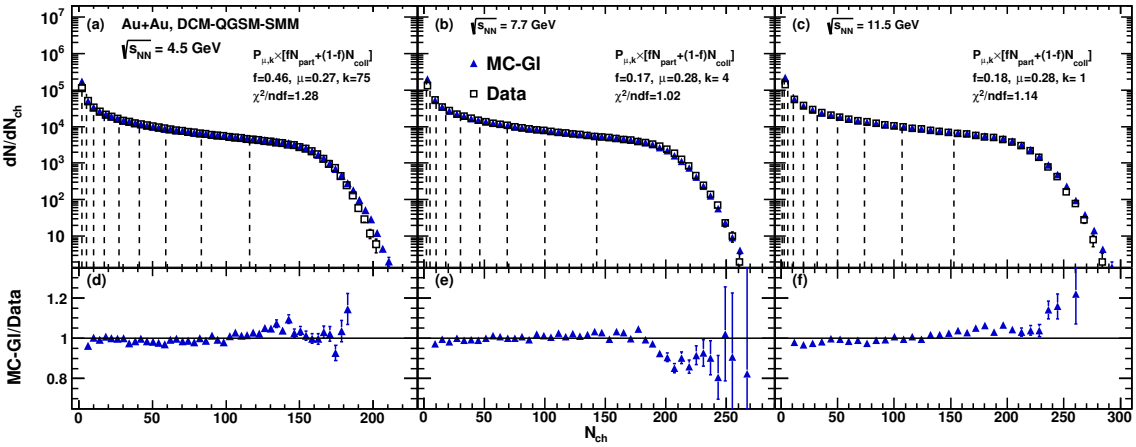

Figure 8: Distribution of the charged particle multiplicity for Au+Au collisions at at $\sqrt{s_{NN}}$=4.5, 7.7 and 11.5 GeV from DCM-QGSM-SMM model (open symbols). The distribution is fitted with the Glauber-based fit function (closed symbols). Vertical lines denote sharp cuts for centrality classes.

θ	N_{knee}	a_1	a_2	a_3	χ^2	NDF	$N_{ch}^{fit}(min)$
1.17	219.67	-4.26	2.08	-3.97	307.03	245.00	20

Table 4: Parameters of the fit to the charged particle multiplicity of the UrQMD model for Au+Au collisions at $\sqrt{s_{NN}}$ =7.7 GeV..

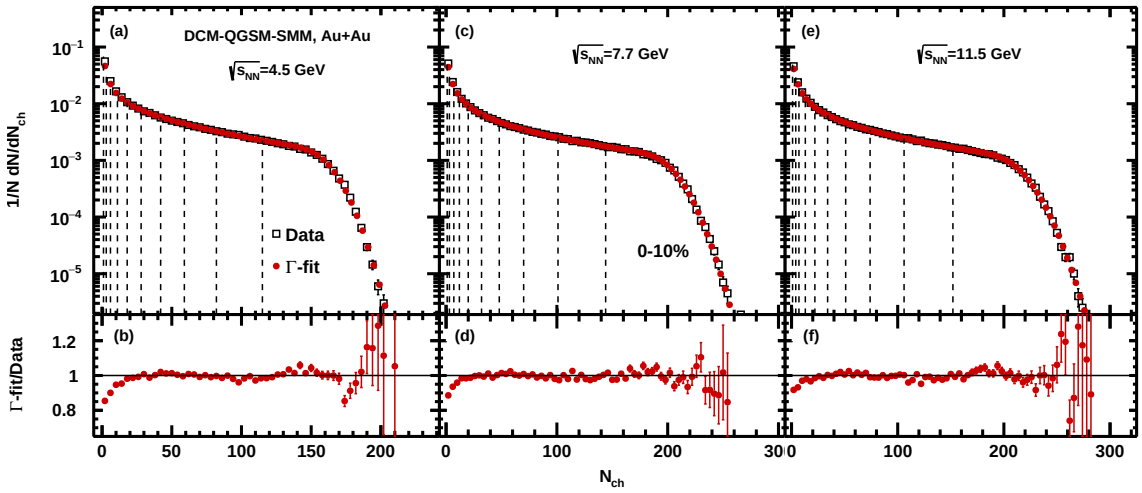

Figure 9: Charged particle multiplicity distribution from the DCM-QGMS-SMM model (open squares) for Au+Au collisions at $\sqrt{s_{NN}}$ =4.5, 7.7 and 11.5 GeV compared to the fitted distribution using Γ-fit (red circles) approach. Bottom plots show ratio of the resulted fit functions to the charged particle multiplicity distribution.

θ	N_{knee}	a_1	a_2	a_3	χ^2	NDF	$N_{ch}^{fit}(min)$
1.24	277.03	-4.25	2.06	-3.93	379.20	310.00	20

Table 5: Parameters of the fit to the charged particle multiplicity of the UrQMD model for Au+Au collisions at $\sqrt{s_{NN}}$ =11.5 GeV.

θ	N_{knee}	a_1	a_2	a_3	χ^2	NDF	$N_{ch}^{fit}(min)$
0.94	120.99	-4.07	2.80	-4.45	185.83	133.00	20

Table 6: Parameters of the fit to the charged particle multiplicity of the AMPT model for Au+Au collisions at $\sqrt{s_{NN}}$ =4.5 GeV.

θ	N_{knee}	a_1	a_2	a_3	χ^2	NDF	$N_{ch}^{fit}(min)$
0.99	211.07	-3.80	1.97	-3.63	294.77	229.00	20

Table 7: Parameters of the fit to the charged particle multiplicity of the AMPT model for Au+Au collisions at $\sqrt{s_{NN}}$ =7.7 GeV..

θ	N_{knee}	a_1	a_2	a_3	χ^2	NDF	$N_{ch}^{fit}(min)$
1.12	257.66	-3.56	1.37	-3.25	328.18	287.00	20

Table 8: Parameters of the fit to the charged particle multiplicity of the AMPT model for Au+Au collisions at $\sqrt{s_{NN}}$ =11.5 GeV.

θ	N_{knee}	a_1	a_2	a_3	χ^2	NDF	$N_{ch}^{fit}(min)$
0.97	164.25	-4.20	2.49	-4.35	207.14	181.00	20

Table 9: Parameters of the fit to the charged particle multiplicity of the DCM-QGMS-SMM model for Au+Au collisions at $\sqrt{s_{NN}}$ =4.5 GeV.

θ	N_{knee}	a_1	a_2	a_3	χ^2	NDF	$N_{ch}^{fit}(min)$
1.32	206.78	-4.12	1.45	-3.19	275.49	235.00	20

Table 10: Parameters of the fit to the charged particle multiplicity of the DCM-QGMS-SMM model for Au+Au collisions at $\sqrt{s_{NN}}$ =7.7 GeV..

θ	N_{knee}	a_1	a_2	a_3	χ^2	NDF	$N_{ch}^{fit}(min)$
1.61	218.78	-4.12	1.68	-3.23	272.40	254.00	20

Table 11: Parameters of the fit to the charged particle multiplicity of the DCM-QGMS-SMM model for Au+Au collisions at $\sqrt{s_{NN}}$ =11.5 GeV.

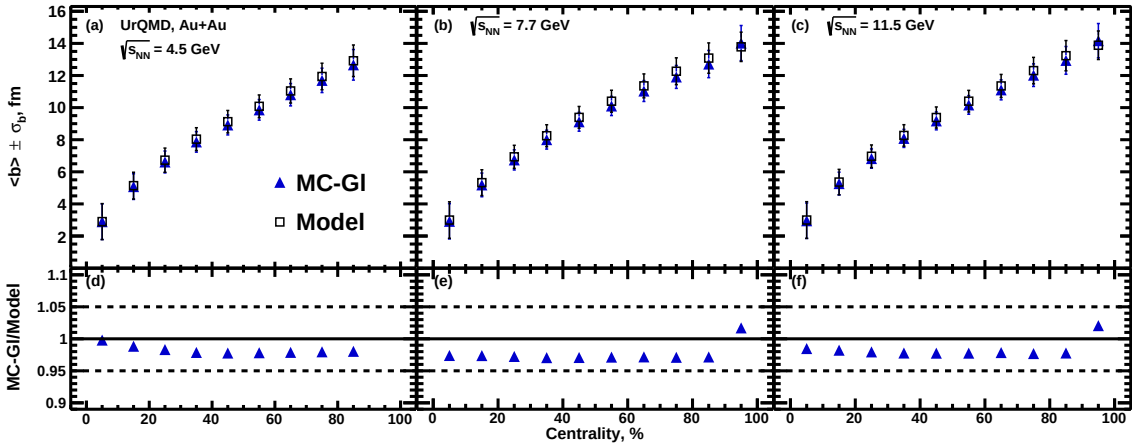

Figure 10: Centrality dependence of $\langle b \rangle$ for Au+Au collisions at at $\sqrt{s_{NN}}$=4.5, 7.7 and 11.5 GeV from MC-Glauber calculations (closed symbols) and UrQMD model (open symbols).

Centrality, %	N_{ch}^{min}	N_{ch}^{max}	$\langle b \rangle$, fm	RMS	b_{min}, fm	b_{max}, fm	$\langle N_{part} \rangle$	RMS	N_{part}^{min}	N_{part}^{max}	$\langle N_{coll} \rangle$	RMS	N_{coll}^{min}	N_{coll}^{max}
0 - 10	108	203	2.89	1.11	1.46	4.08	318.54	32.37	279.34	362.01	673.60	88.84	566.43	798.75
10 - 20	77	108	5.08	0.80	4.08	5.90	244.20	30.80	212.53	279.34	474.69	73.41	396.03	566.43
20 - 30	54	77	6.61	0.68	5.90	7.27	184.53	26.27	159.56	212.53	329.60	57.84	272.25	396.03
30 - 40	37	54	7.86	0.64	7.27	8.40	137.24	22.39	117.94	159.56	223.34	45.44	182.96	272.25
40 - 50	25	37	8.92	0.62	8.40	9.40	100.53	18.86	85.14	117.94	148.03	34.92	118.87	182.96
50 - 60	16	25	9.86	0.64	9.40	10.34	71.76	16.19	58.96	85.14	94.84	27.24	73.22	118.87
60 - 70	9	16	10.80	0.70	10.34	11.24	47.49	13.78	38.00	58.96	55.30	20.48	41.45	73.22
70 - 80	5	9	11.70	0.76	11.24	12.17	29.46	10.80	22.00	38.00	29.98	13.86	20.89	41.45
80 - 90	2	5	12.67	0.95	12.17	13.21	16.18	8.50	12.29	22.00	14.41	9.28	10.45	20.89

Table 12: Geometric properties (b, N_{part}, N_{coll}) of Au+Au collisions at $\sqrt{s_{NN}}$=4.5 GeV from UrQMD model for centrality classes defined by sharp cuts in the charged particle multiplicity distribution, simulated with an NBD-Glauber fit. The mean values and the RMS are obtained with a Glauber Monte Carlo calculation.

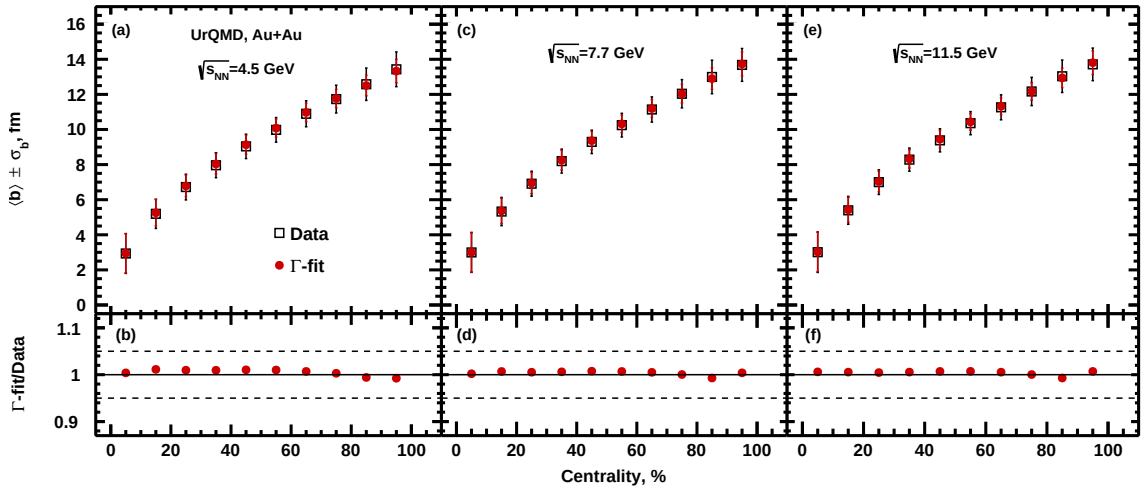

Figure 11: Centrality dependence of the average impact parameter $\langle b \rangle$ for Au+Au collisions at $\sqrt{s_{NN}}$=4.5, 7.7 and 11.5 GeV for Γ-fit approach. The resulting values of $\langle b \rangle$ extracted from the Γ-fit approach (red circles) are compared with the values used in UrQMD model (open symbols). Centrality was based on N_{ch} for charged particle within $|\eta| < 0.5$ and $p_T > 0.15$ GeV/c.

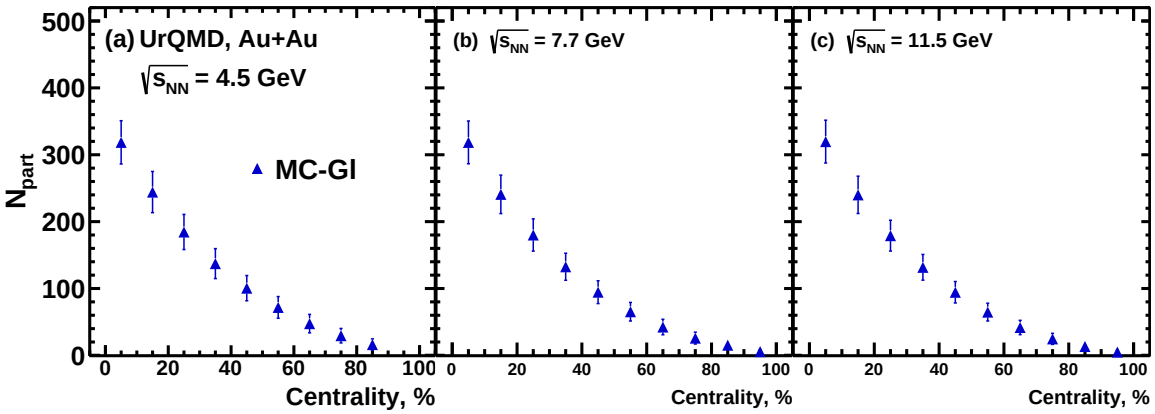

Figure 12: Centrality dependence of $\langle N_{part} \rangle$ for Au+Au collisions at at $\sqrt{s_{NN}}$=4.5, 7.7 and 11.5 GeV from MC-Glauber calculations (closed symbols) and UrQMD model (open symbols).

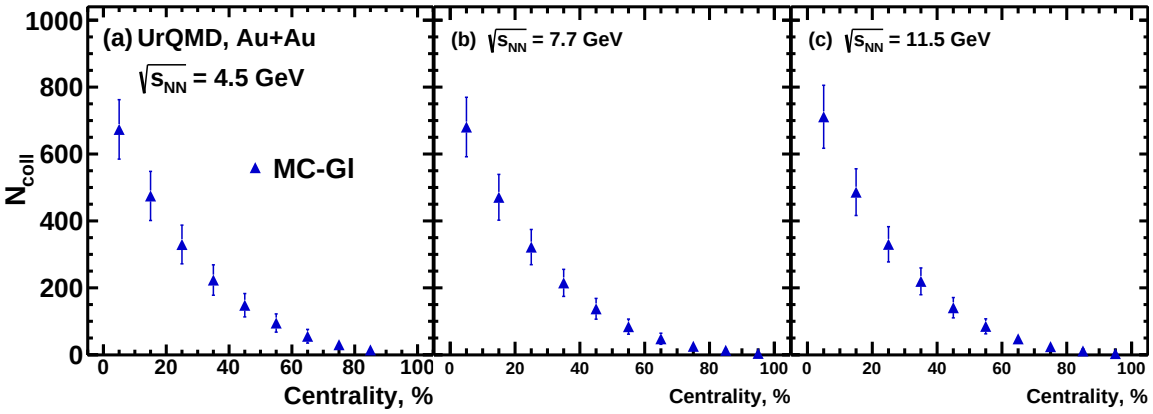

Figure 13: Centrality dependence of $\langle N_{coll} \rangle$ for Au+Au collisions at at $\sqrt{s_{NN}}$=4.5, 7.7 and 11.5 GeV from MC-Glauber calculations (closed symbols) and UrQMD model (open symbols).

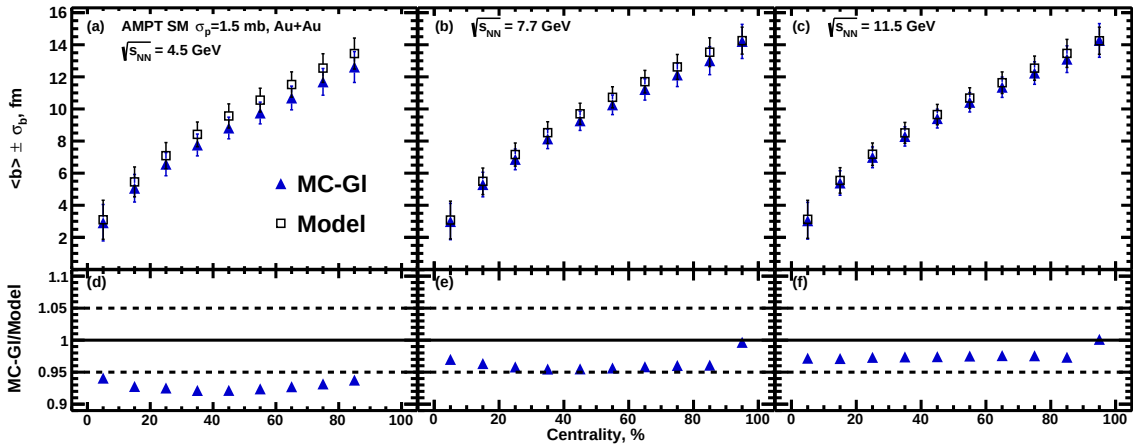

Figure 14: Centrality dependence of $\langle b \rangle$ for Au+Au collisions at at $\sqrt{s_{NN}}$=4.5, 7.7 and 11.5 GeV from MC-Glauber calculations (closed symbols) and AMPT SM model with σ_p=1.5 mb model (open symbols).

Centrality, %	N_{ch}^{min}	N_{ch}^{max}	$\langle b \rangle$, fm	RMS	b_{min}, fm	b_{max}, fm	$\langle N_{part} \rangle$	RMS	N_{part}^{min}	N_{part}^{max}	$\langle N_{coll} \rangle$	RMS	N_{coll}^{min}	N_{coll}^{max}
0 - 10	85	163	2.91	1.14	1.54	4.07	317.83	33.32	279.51	359.69	671.38	91.82	566.67	792.22
10 - 20	61	85	5.06	0.86	4.07	5.86	244.79	32.79	214.11	279.51	476.37	79.68	400.15	566.67
20 - 30	44	61	6.56	0.72	5.86	7.20	186.62	27.71	162.35	214.11	334.56	62.46	278.85	400.15
30 - 40	31	44	7.76	0.68	7.20	8.29	141.29	24.10	121.71	162.35	232.27	50.37	190.84	278.85
40 - 50	21	31	8.81	0.67	8.29	9.27	104.19	20.90	89.17	121.71	155.52	40.04	126.51	190.84
50 - 60	14	21	9.75	0.68	9.27	10.23	75.10	17.68	62.19	89.17	100.91	30.73	78.88	126.51
60 - 70	8	14	10.68	0.74	10.23	11.19	50.50	15.44	39.54	62.19	60.17	23.78	44.00	78.88
70 - 80	4	8	11.69	0.83	11.19	12.15	29.98	12.33	22.29	39.54	30.94	16.18	21.25	44.00
80 - 90	2	4	12.61	0.96	12.15	13.08	16.87	9.08	14.68	22.29	15.24	10.18	13.73	21.25

Table 13: Geometric properties (b, N_{part}, N_{coll}) of Au+Au collisions at $\sqrt{s_{NN}}$=4.5 GeV from AMPT SM model with σ_p=1.5 mb for centrality classes defined by sharp cuts in the charged particle multiplicity distribution, simulated with an NBD-Glauber fit. The mean values and the RMS are obtained with a Glauber Monte Carlo calculation.

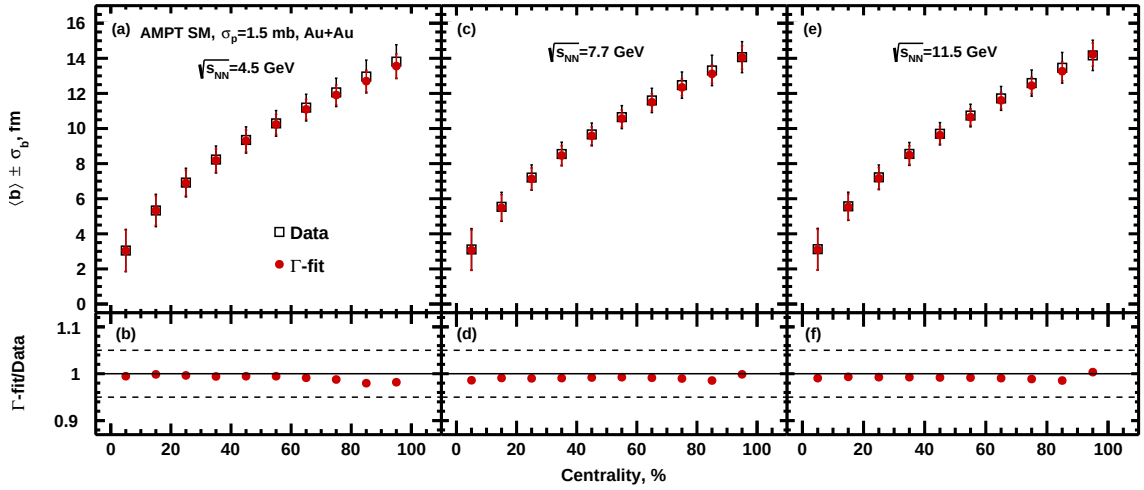

Figure 15: Centrality dependence of the average impact parameter $\langle b \rangle$ for Au+Au collisions at $\sqrt{s_{NN}}$=4.5, 7.7 and 11.5 GeV for Γ-fit approach. The resulting values of $\langle b \rangle$ extracted from the Γ-fit approach (red circles) are compared with the values used in AMPT model (open symbols). Centrality was based on N_{ch} for charged particle within $|\eta| < 0.5$ and $p_T > 0.15$ GeV/c.

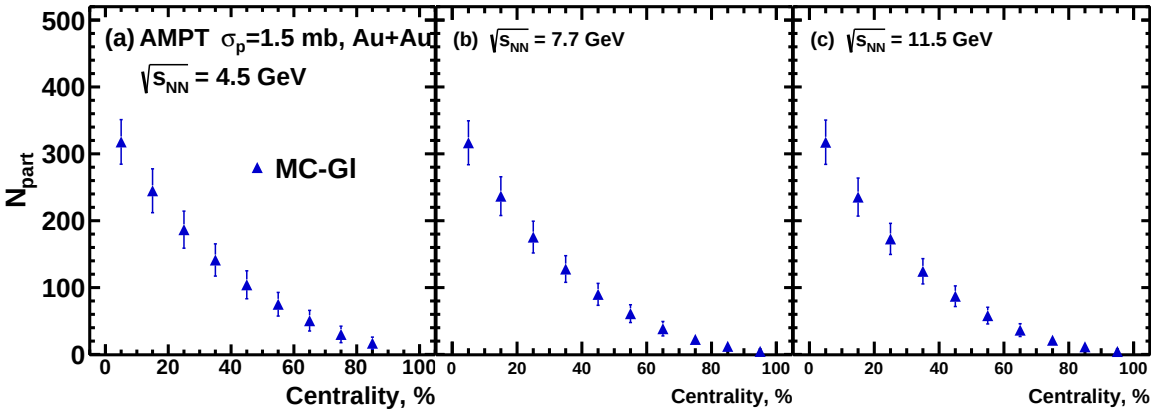

Figure 16: Centrality dependence of $\langle N_{part} \rangle$ for Au+Au collisions at at $\sqrt{s_{NN}}$=4.5, 7.7 and 11.5 GeV from MC-Glauber calculations (closed symbols) and AMPT SM model with σ_p=1.5 mb model (open symbols).

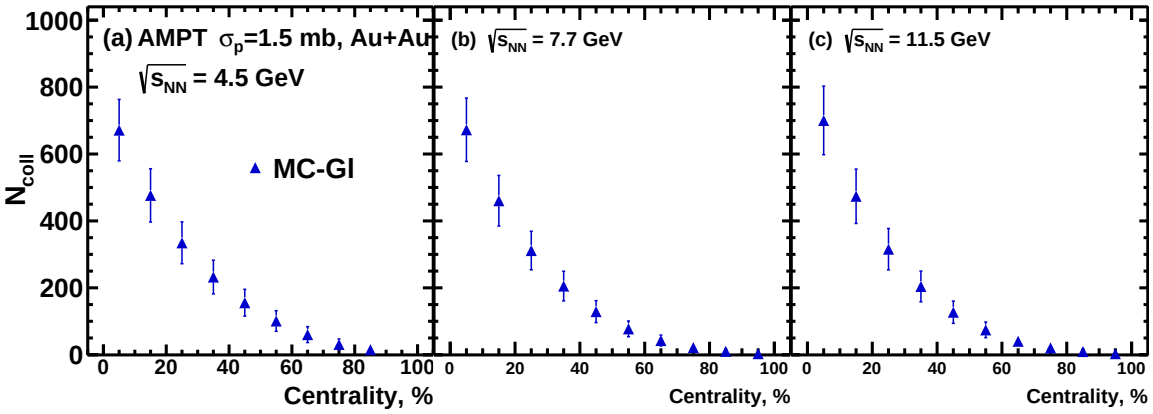

Figure 17: Centrality dependence of $\langle N_{coll} \rangle$ for Au+Au collisions at at $\sqrt{s_{NN}}$=4.5, 7.7 and 11.5 GeV from MC-Glauber calculations (closed symbols) and AMPT SM model with σ_p=1.5 mb model (open symbols).

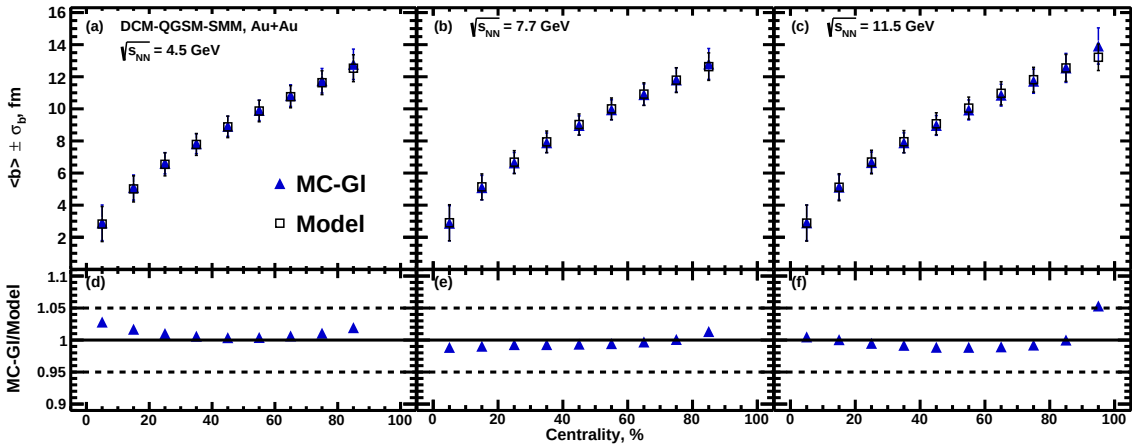

Figure 18: Centrality dependence of $\langle b \rangle$ for Au+Au collisions at at $\sqrt{s_{NN}}$=4.5, 7.7 and 11.5 GeV from MC-Glauber calculations (closed symbols) and DCM-QGSM-SMM model (open symbols).

Centrality, %	N_{ch}^{min}	N_{ch}^{max}	$\langle b \rangle$, fm	RMS	b_{min}, fm	b_{max}, fm	$\langle N_{part} \rangle$	RMS	N_{part}^{min}	N_{part}^{max}	$\langle N_{coll} \rangle$	RMS	N_{coll}^{min}	N_{coll}^{max}
0 - 10	116	210	2.90	1.11	1.39	4.11	318.30	32.31	278.43	363.93	672.70	88.86	564.46	800.74
10 - 20	83	116	5.10	0.78	4.11	5.91	243.49	30.10	212.41	278.43	472.85	72.00	395.81	564.46
20 - 30	59	83	6.61	0.66	5.91	7.25	184.67	25.50	160.34	212.41	329.81	56.26	273.71	395.81
30 - 40	41	59	7.83	0.62	7.25	8.38	138.52	21.80	118.59	160.34	226.06	44.55	184.18	273.71
40 - 50	27	41	8.91	0.62	8.38	9.41	100.86	18.83	84.90	118.59	148.66	35.15	118.54	184.18
50 - 60	17	27	9.90	0.64	9.41	10.38	70.48	15.75	57.98	84.90	92.61	26.50	71.63	118.54
60 - 70	10	17	10.83	0.67	10.38	11.29	46.91	13.03	37.01	57.98	54.37	19.32	39.98	71.63
70 - 80	5	10	11.75	0.76	11.29	12.23	28.49	10.57	21.21	37.01	28.77	13.45	20.09	39.98
80 - 90	2	5	12.78	0.95	12.23	13.43	14.90	7.80	9.34	21.21	13.00	8.31	6.58	20.09

Table 14: Geometric properties (b, N_{part}, N_{coll}) of Au+Au collisions at $\sqrt{s_{NN}}$=4.5 GeV from DCM-QGSM-SMM model for centrality classes defined by sharp cuts in the charged particle multiplicity distribution, simulated with an NBD-Glauber fit. The mean values and the RMS are obtained with a Glauber Monte Carlo calculation.

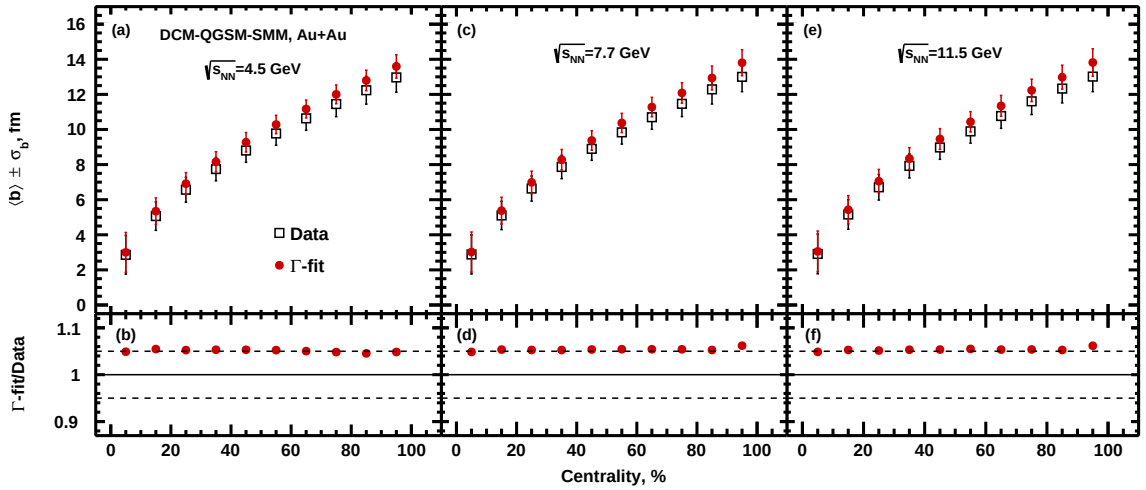

Figure 19: Centrality dependence of the average impact parameter $\langle b \rangle$ for Au+Au collisions at $\sqrt{s_{NN}}$=4.5, 7.7 and 11.5 GeV for Γ-fit approach. The resulting values of $\langle b \rangle$ extracted from the Γ-fit approach (red circles) are compared with the values used in DCM-QGMS-SMM model (open symbols). Centrality was based on N_{ch} for charged particle within $|\eta| < 0.5$ and $p_T > 0.15$ GeV/c.

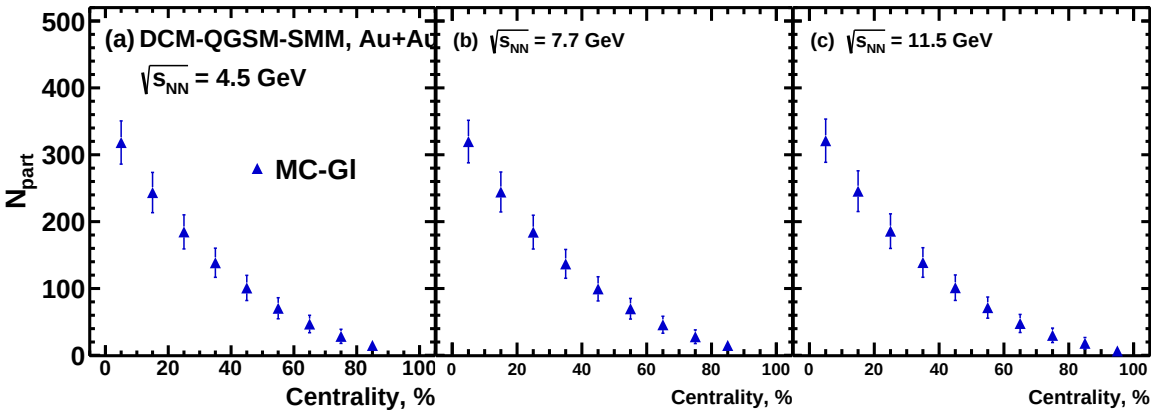

Figure 20: Centrality dependence of $\langle N_{part} \rangle$ for Au+Au collisions at at $\sqrt{s_{NN}}$=4.5, 7.7 and 11.5 GeV from MC-Glauber calculations (closed symbols) and DCM-QGSM-SMM model (open symbols).

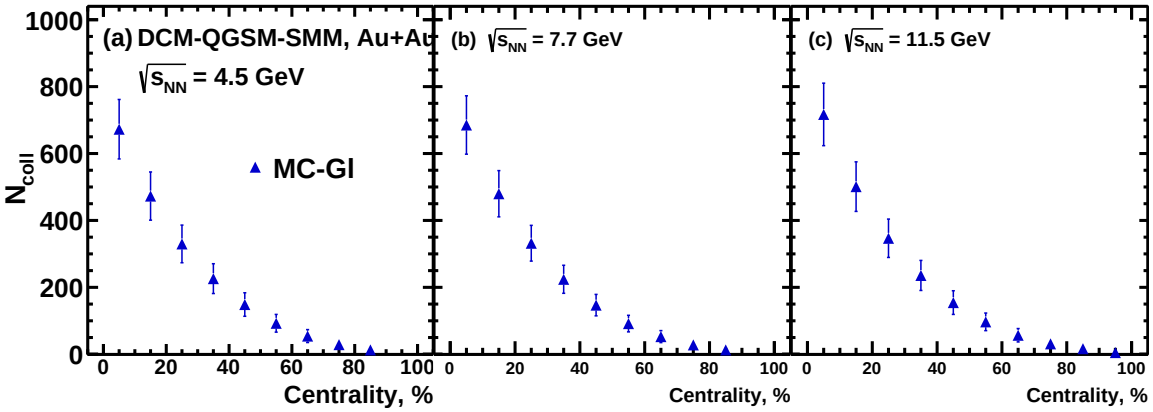

Figure 21: Centrality dependence of $\langle N_{coll} \rangle$ for Au+Au collisions at at $\sqrt{s_{NN}}$=4.5, 7.7 and 11.5 GeV from MC-Glauber calculations (closed symbols) and DCM-QGSM-SMM model (open symbols).

Centrality, %	N_{ch}^{min}	N_{ch}^{max}	$\langle b \rangle$, fm	RMS	b_{min}, fm	b_{max}, fm	$\langle N_{part} \rangle$	RMS	N_{part}^{min}	N_{part}^{max}	$\langle N_{coll} \rangle$	RMS	N_{coll}^{min}	N_{coll}^{max}
0 - 10	152	280	2.92	1.10	1.31	4.17	318.50	31.96	276.69	367.71	680.71	88.89	566.73	816.48
10 - 20	107	152	5.19	0.74	4.17	6.03	240.81	28.75	208.31	276.69	470.67	68.42	389.88	566.73
20 - 30	74	107	6.74	0.63	6.03	7.40	180.04	24.10	155.13	208.31	321.82	52.63	263.69	389.88
30 - 40	50	74	8.01	0.59	7.40	8.56	132.53	20.22	112.75	155.13	214.83	40.43	173.08	263.69
40 - 50	32	50	9.12	0.59	8.56	9.63	94.54	17.06	78.92	112.75	137.34	31.06	108.41	173.08
50 - 60	20	32	10.10	0.60	9.63	10.59	65.30	13.85	52.68	78.92	84.03	22.55	63.71	108.41
60 - 70	11	20	11.03	0.65	10.59	11.46	42.42	11.59	33.45	52.68	47.80	16.56	35.00	63.71
70 - 80	6	11	11.91	0.71	11.46	12.29	25.83	8.85	20.19	33.45	25.33	10.85	18.48	35.00
80 - 90	3	6	12.71	0.85	12.29	13.30	15.27	6.80	10.49	20.19	13.28	7.21	8.85	18.48
90 - 100	1	2	14.02	1.09	13.30	14.94	5.63	3.77	-0.30	10.49	4.12	3.33	-2.46	8.85

Table 15: Geometric properties (b, N_{part}, N_{coll}) of Au+Au collisions at $\sqrt{s_{NN}}$=7.7 GeV from UrQMD model for centrality classes defined by sharp cuts in the charged particle multiplicity distribution, simulated with an NBD-Glauber fit. The mean values and the RMS are obtained with a Glauber Monte Carlo calculation.

Centrality, %	N_{ch}^{min}	N_{ch}^{max}	$\langle b \rangle$, fm	RMS	b_{min}, fm	b_{max}, fm	$\langle N_{part} \rangle$	RMS	N_{part}^{min}	N_{part}^{max}	$\langle N_{coll} \rangle$	RMS	N_{coll}^{min}	N_{coll}^{max}
0 - 10	151	270	2.99	1.13	1.41	4.25	316.55	32.83	273.76	366.37	672.49	94.68	557.63	808.12
10 - 20	109	151	5.29	0.77	4.25	6.14	236.72	28.98	204.04	273.76	460.38	75.58	379.74	557.63
20 - 30	78	109	6.86	0.65	6.14	7.53	175.52	23.77	150.23	204.04	311.49	57.56	253.43	379.74
30 - 40	54	78	8.14	0.61	7.53	8.71	127.78	19.91	107.91	150.23	205.26	44.25	163.82	253.43
40 - 50	36	54	9.26	0.60	8.71	9.77	89.90	16.41	74.53	107.91	128.93	32.82	100.86	163.82
50 - 60	23	36	10.26	0.61	9.77	10.76	61.05	13.30	48.76	74.53	77.37	23.46	57.95	100.86
60 - 70	13	23	11.21	0.66	10.76	11.66	38.54	10.79	29.82	48.76	42.58	16.22	30.58	57.95
70 - 80	7	13	12.12	0.73	11.66	12.55	22.52	7.92	16.85	29.82	21.53	9.94	14.95	30.58
80 - 90	3	7	13.01	0.87	12.55	13.56	12.19	5.66	8.20	16.85	10.21	5.95	6.60	14.95
90 - 100	1	2	14.21	1.06	13.56	15.02	4.60	2.70	0.78	8.20	3.26	2.38	-0.92	6.60

Table 16: Geometric properties (b, N_{part}, N_{coll}) of Au+Au collisions at $\sqrt{s_{NN}}$=7.7 GeV from AMPT SM model with σ_p=1.5 mb for centrality classes defined by sharp cuts in the charged particle multiplicity distribution, simulated with an NBD-Glauber fit. The mean values and the RMS are obtained with a Glauber Monte Carlo calculation.

Centrality, %	N_{ch}^{min}	N_{ch}^{max}	$\langle b \rangle$, fm	RMS	b_{min}, fm	b_{max}, fm	$\langle N_{part} \rangle$	RMS	N_{part}^{min}	N_{part}^{max}	$\langle N_{coll} \rangle$	RMS	N_{coll}^{min}	N_{coll}^{max}
0 - 10	143	262	2.87	1.09	1.38	4.09	319.73	31.80	279.78	364.69	685.29	87.23	574.16	816.42
10 - 20	100	143	5.09	0.76	4.09	5.92	244.33	29.88	212.52	279.78	479.84	69.09	399.69	574.16
20 - 30	69	100	6.63	0.65	5.92	7.29	184.32	25.29	159.30	212.52	331.87	53.44	273.71	399.69
30 - 40	46	69	7.89	0.61	7.29	8.44	136.84	21.55	117.14	159.30	224.10	41.89	182.50	273.71
40 - 50	30	46	8.97	0.60	8.44	9.46	99.49	18.11	83.65	117.14	146.87	32.05	116.74	182.50
50 - 60	18	30	9.94	0.62	9.46	10.42	69.75	15.42	57.07	83.65	91.65	24.74	70.26	116.74
60 - 70	10	18	10.89	0.66	10.42	11.34	45.82	12.69	36.26	57.07	52.74	17.97	38.93	70.26
70 - 80	5	10	11.80	0.76	11.34	12.28	27.89	10.23	20.70	36.26	27.95	12.54	19.42	38.93
80 - 90	2	5	12.80	0.96	12.28	13.39	14.88	7.84	10.49	20.70	12.97	8.17	7.99	19.42

Table 17: Geometric properties (b, N_{part}, N_{coll}) of Au+Au collisions at $\sqrt{s_{NN}}$=7.7 GeV from DCM-QGSM-SMM model for centrality classes defined by sharp cuts in the charged particle multiplicity distribution, simulated with an NBD-Glauber fit. The mean values and the RMS are obtained with a Glauber Monte Carlo calculation.

Centrality, %	N_{ch}^{min}	N_{ch}^{max}	$\langle b \rangle$, fm	RMS	b_{min}, fm	b_{max}, fm	$\langle N_{part} \rangle$	RMS	N_{part}^{min}	N_{part}^{max}	$\langle N_{coll} \rangle$	RMS	N_{coll}^{min}	N_{coll}^{max}
0 - 10	191	335	2.95	1.10	1.35	4.23	319.67	31.99	276.85	369.85	711.32	94.14	588.81	856.96
10 - 20	134	191	5.27	0.71	4.23	6.11	240.05	27.89	207.43	276.85	486.03	69.79	401.46	588.81
20 - 30	93	134	6.83	0.60	6.11	7.49	179.04	23.03	154.10	207.43	330.11	52.68	269.79	401.46
30 - 40	63	93	8.08	0.56	7.49	8.63	131.69	19.21	112.07	154.10	219.43	40.06	176.50	269.79
40 - 50	41	63	9.17	0.56	8.63	9.68	94.40	16.02	78.61	112.07	140.58	30.37	110.33	176.50
50 - 60	25	41	10.17	0.58	9.68	10.65	64.72	13.28	52.32	78.61	84.95	22.40	64.38	110.33
60 - 70	14	25	11.11	0.62	10.65	11.56	41.70	10.69	32.51	52.32	47.59	15.68	34.34	64.38
70 - 80	7	14	12.02	0.70	11.56	12.46	24.71	8.25	18.48	32.51	24.27	10.20	16.75	34.34
80 - 90	3	7	12.94	0.86	12.46	13.50	13.30	6.00	8.88	18.48	11.33	6.20	7.27	16.75
90 - 100	1	2	14.17	1.07	13.50	15.00	4.97	3.05	1.02	8.88	3.55	2.64	-1.06	7.27

Table 18: Geometric properties (b, N_{part}, N_{coll}) of Au+Au collisions at $\sqrt{s_{NN}}$=11.5 GeV from UrQMD model for centrality classes defined by sharp cuts in the charged particle multiplicity distribution, simulated with an NBD-Glauber fit. The mean values and the RMS are obtained with a Glauber Monte Carlo calculation.

Centrality, %	N_{ch}^{min}	N_{ch}^{max}	$\langle b \rangle$, fm	RMS	b_{min}, fm	b_{max}, fm	$\langle N_{part} \rangle$	RMS	N_{part}^{min}	N_{part}^{max}	$\langle N_{coll} \rangle$	RMS	N_{coll}^{min}	N_{coll}^{max}
0 - 10	185	317	3.04	1.15	1.42	4.33	317.38	33.12	273.34	368.72	700.42	102.51	577.44	845.64
10 - 20	135	185	5.39	0.76	4.33	6.25	235.35	28.44	201.88	273.34	473.73	81.28	387.92	577.44
20 - 30	97	135	6.99	0.65	6.25	7.67	172.80	23.24	147.19	201.88	315.55	61.72	254.79	387.92
30 - 40	68	97	8.29	0.60	7.67	8.85	124.38	18.91	104.65	147.19	204.22	45.83	161.91	254.79
40 - 50	46	68	9.40	0.59	8.85	9.92	87.10	15.43	71.55	104.65	127.11	33.32	98.02	161.91
50 - 60	29	46	10.41	0.60	9.92	10.90	58.11	12.48	46.35	71.55	74.36	23.34	55.48	98.02
60 - 70	17	29	11.35	0.63	10.90	11.80	36.42	9.57	28.14	46.35	40.36	15.02	28.93	55.48
70 - 80	9	17	12.24	0.70	11.80	12.66	21.31	7.03	15.88	28.14	20.38	9.10	14.05	28.93
80 - 90	4	9	13.10	0.83	12.66	13.63	11.50	4.86	7.82	15.88	9.57	5.15	6.22	14.05
90 - 100	1	3	14.27	1.05	13.63	15.07	4.45	2.44	0.80	7.82	3.13	2.13	-0.69	6.22

Table 19: Geometric properties (b, N_{part}, N_{coll}) of Au+Au collisions at $\sqrt{s_{NN}}$=11.5 GeV from AMPT SM model with σ_p=1.5 mb for centrality classes defined by sharp cuts in the charged particle multiplicity distribution, simulated with an NBD-Glauber fit. The mean values and the RMS are obtained with a Glauber Monte Carlo calculation.

Centrality, %	N_{ch}^{min}	N_{ch}^{max}	$\langle b \rangle$, fm	RMS	b_{min}, fm	b_{max}, fm	$\langle N_{part} \rangle$	RMS	N_{part}^{min}	N_{part}^{max}	$\langle N_{coll} \rangle$	RMS	N_{coll}^{min}	N_{coll}^{max}
0 - 10	153	281	2.90	1.11	1.32	4.13	321.04	32.33	280.35	368.94	716.92	93.40	599.50	857.65
10 - 20	107	153	5.12	0.78	4.13	5.95	245.55	30.47	213.61	280.35	501.06	74.07	417.24	599.50
20 - 30	74	107	6.65	0.66	5.95	7.29	185.77	25.86	161.37	213.61	346.70	57.33	286.75	417.24
30 - 40	50	74	7.89	0.62	7.29	8.43	138.89	22.11	119.32	161.37	235.61	44.89	192.05	286.75
40 - 50	32	50	8.97	0.62	8.43	9.47	101.24	19.05	85.31	119.32	154.45	35.37	123.26	192.05
50 - 60	20	32	9.93	0.62	9.47	10.42	71.45	15.82	58.47	85.31	96.88	26.30	74.58	123.26
60 - 70	11	20	10.85	0.68	10.42	11.27	47.73	13.53	38.28	58.47	56.83	20.00	42.36	74.58
70 - 80	6	11	11.72	0.75	11.27	12.11	30.00	10.80	23.74	38.28	31.14	13.79	22.99	42.36
80 - 90	3	6	12.55	0.90	12.11	13.17	18.10	8.63	12.43	23.74	16.61	9.57	11.00	22.99
90 - 100	1	2	13.92	1.13	13.17	14.88	6.63	4.90	-0.33	12.43	5.04	4.51	-3.01	11.00

Table 20: Geometric properties (b, N_{part}, N_{coll}) of Au+Au collisions at $\sqrt{s_{NN}}$=11.5 GeV from DCM-QGSM-SMM model for centrality classes defined by sharp cuts in the charged particle multiplicity distribution, simulated with an NBD-Glauber fit. The mean values and the RMS are obtained with a Glauber Monte Carlo calculation.

Centrality, %	N_{ch}^{min}	N_{ch}^{max}	$\langle b \rangle$, fm	RMS	b_{min}, fm	b_{max}, fm
0 - 10	107	206	2.95	1.11	1.40	4.21
10 - 20	76	107	5.25	0.75	4.21	6.08
20 - 30	55	76	6.78	0.61	6.08	7.45
30 - 40	38	55	8.04	0.58	7.45	8.59
40 - 50	26	38	9.13	0.53	8.59	9.61
50 - 60	17	26	10.08	0.51	9.61	10.54
60 - 70	10	17	10.97	0.52	10.54	11.38
70 - 80	6	10	11.77	0.52	11.38	12.14
80 - 90	3	6	12.51	0.58	12.14	12.89
90 - 100	1	3	13.33	0.67	12.89	13.86

Table 21: The centrality clases, the mean value of impact parameter and the RMS from the UrQMD model for Au+Au collisions at $\sqrt{s_{NN}}$ =4.5 GeV from Γ-fit approach.

Centrality, %	N_{ch}^{min}	N_{ch}^{max}	$\langle b \rangle$, fm	RMS	b_{min}, fm	b_{max}, fm
0 - 10	86	177	3.03	1.17	1.57	4.27
10 - 20	63	86	5.32	0.83	4.27	6.16
20 - 30	46	63	6.89	0.72	6.16	7.59
30 - 40	33	46	8.19	0.66	7.59	8.75
40 - 50	23	33	9.30	0.62	8.75	9.77
50 - 60	16	23	10.24	0.57	9.77	10.68
60 - 70	10	16	11.09	0.57	10.68	11.51
70 - 80	6	10	11.91	0.57	11.51	12.30
80 - 90	3	6	12.70	0.62	12.30	13.11
90 - 100	1	3	13.56	0.69	13.11	14.09

Table 22: The centrality clases, the mean value of impact parameter and the RMS from the AMPT model for Au+Au collisions at $\sqrt{s_{NN}}$ =4.5 GeV from Γ-fit approach.

Centrality, %	N_{ch}^{min}	N_{ch}^{max}	$\langle b \rangle$, fm	RMS	b_{min}, fm	b_{max}, fm
0 - 10	115	221	3.00	1.13	1.42	4.29
10 - 20	82	115	5.34	0.76	4.29	6.18
20 - 30	59	82	6.91	0.63	6.18	7.58
30 - 40	42	59	8.16	0.58	7.58	8.73
40 - 50	28	42	9.27	0.55	8.73	9.77
50 - 60	18	28	10.28	0.52	9.77	10.74
60 - 70	11	18	11.17	0.51	10.74	11.61
70 - 80	6	11	12.00	0.53	11.61	12.40
80 - 90	3	6	12.79	0.58	12.40	13.17
90 - 100	1	3	13.59	0.67	13.17	14.11

Table 23: The centrality clases, the mean value of impact parameter and the RMS from the DCM-QGMS-SMM model for Au+Au collisions at $\sqrt{s_{NN}}$ =4.5 GeV from Γ-fit approach.

Centrality, %	N_{ch}^{min}	N_{ch}^{max}	$\langle b \rangle$, fm	RMS	b_{min}, fm	b_{max}, fm
0 - 10	152	287	3.02	1.13	1.53	4.30
10 - 20	107	152	5.39	0.73	4.30	6.24
20 - 30	75	107	6.99	0.61	6.24	7.70
30 - 40	51	75	8.30	0.56	7.70	8.87
40 - 50	34	51	9.42	0.52	8.87	9.89
50 - 60	22	34	10.38	0.50	9.89	10.83
60 - 70	13	22	11.26	0.51	10.83	11.70
70 - 80	7	13	12.11	0.53	11.70	12.54
80 - 90	3	7	12.98	0.62	12.54	13.38
90 - 100	1	3	13.82	0.68	13.38	14.31

Table 24: The centrality clases, the mean value of impact parameter and the RMS from the UrQMD model for Au+Au collisions at $\sqrt{s_{NN}}$ =7.7 GeV from Γ-fit approach.

Centrality, %	N_{ch}^{min}	N_{ch}^{max}	$\langle b \rangle$, fm	RMS	b_{min}, fm	b_{max}, fm
0 - 10	150	274	3.07	1.15	1.42	4.40
10 - 20	108	150	5.49	0.74	4.40	6.38
20 - 30	77	108	7.14	0.62	6.38	7.84
30 - 40	54	77	8.47	0.55	7.84	9.03
40 - 50	37	54	9.59	0.51	9.03	10.09
50 - 60	24	37	10.57	0.48	10.09	11.06
60 - 70	14	24	11.50	0.48	11.06	11.93
70 - 80	8	14	12.34	0.48	11.93	12.73
80 - 90	4	8	13.12	0.53	12.73	13.56
90 - 100	1	4	14.05	0.66	13.56	14.64

Table 25: The centrality clases, the mean value of impact parameter and the RMS from the AMPT model for Au+Au collisions at $\sqrt{s_{NN}}$ =7.7 GeV from Γ-fit approach.

Centrality, %	N_{ch}^{min}	N_{ch}^{max}	$\langle b \rangle$, fm	RMS	b_{min}, fm	b_{max}, fm
0 - 10	144	282	3.02	1.14	1.46	4.31
10 - 20	101	144	5.38	0.76	4.31	6.24
20 - 30	70	101	6.98	0.64	6.24	7.67
30 - 40	48	70	8.28	0.58	7.67	8.84
40 - 50	32	48	9.37	0.55	8.84	9.88
50 - 60	20	32	10.37	0.55	9.88	10.83
60 - 70	12	20	11.28	0.55	10.83	11.70
70 - 80	7	12	12.08	0.58	11.70	12.51
80 - 90	3	7	12.93	0.68	12.51	13.34
90 - 100	1	3	13.80	0.74	13.34	14.37

Table 26: The centrality clases, the mean value of impact parameter and the RMS from the DCM-QGMS-SMM model for Au+Au collisions at $\sqrt{s_{NN}}$ =7.7 GeV from Γ-fit approach.

Centrality, %	N_{ch}^{min}	N_{ch}^{max}	$\langle b \rangle$, fm	RMS	b_{min}, fm	b_{max}, fm
0 - 10	190	374	3.03	1.12	1.43	4.34
10 - 20	133	190	5.42	0.70	4.34	6.29
20 - 30	92	133	7.03	0.59	6.29	7.72
30 - 40	63	92	8.33	0.52	7.72	8.90
40 - 50	41	63	9.45	0.50	8.90	9.94
50 - 60	26	41	10.43	0.47	9.94	10.90
60 - 70	15	26	11.32	0.48	10.90	11.76
70 - 80	8	15	12.17	0.50	11.76	12.55
80 - 90	4	8	12.94	0.56	12.55	13.35
90 - 100	1	4	13.81	0.67	13.35	14.35

Table 27: The centrality clases, the mean value of impact parameter and the RMS from the UrQMD model for Au+Au collisions at $\sqrt{s_{NN}}$ =11.5 GeV from Γ-fit approach.

Centrality, %	N_{ch}^{min}	N_{ch}^{max}	$\langle b \rangle$, fm	RMS	b_{min}, fm	b_{max}, fm
0 - 10	185	334	3.10	1.16	1.43	4.44
10 - 20	134	185	5.53	0.73	4.44	6.41
20 - 30	96	134	7.17	0.60	6.41	7.86
30 - 40	67	96	8.49	0.53	7.86	9.07
40 - 50	45	67	9.62	0.49	9.07	10.15
50 - 60	28	45	10.65	0.47	10.15	11.14
60 - 70	16	28	11.61	0.47	11.14	12.04
70 - 80	9	16	12.45	0.47	12.04	12.85
80 - 90	4	9	13.27	0.54	12.85	13.70
90 - 100	1	4	14.22	0.66	13.70	14.85

Table 28: The centrality clases, the mean value of impact parameter and the RMS from the AMPT model for Au+Au collisions at $\sqrt{s_{NN}}$ =11.5 GeV from Γ-fit approach.

Centrality, %	N_{ch}^{min}	N_{ch}^{max}	$\langle b \rangle$, fm	RMS	b_{min}, fm	b_{max}, fm
0 - 10	152	298	3.05	1.16	1.45	4.35
10 - 20	106	152	5.43	0.80	4.35	6.30
20 - 30	74	106	7.05	0.67	6.30	7.74
30 - 40	51	74	8.35	0.62	7.74	8.91
40 - 50	34	51	9.46	0.59	8.91	9.95
50 - 60	22	34	10.44	0.58	9.95	10.91
60 - 70	13	22	11.34	0.60	10.91	11.79
70 - 80	7	13	12.23	0.64	11.79	12.60
80 - 90	4	7	12.98	0.68	12.60	13.39
90 - 100	1	4	13.82	0.78	13.39	14.29

Table 29: The centrality clases, the mean value of impact parameter and the RMS from the DCM-QGMS-SMM model for Au+Au collisions at $\sqrt{s_{NN}}$ =11.5 GeV from Γ-fit approach.

4.2 Reconstructed Au+Au collisions at $\sqrt{s_{NN}}$=7.7 GeV

In this reconstructed data set, UrQMD model together with GEANT4 were used for Au+Au event generation at $\sqrt{s_{NN}}$ = 7.7 GeV and simulation of detector response in the MPD subsystems. Information provided from GEANT4 was reconstructed using dedicated reconstruction tools in MPDROOT framework. This data set was produced during the official production (Request 9 for PWG3) with full reaction plane rotation and 80 ps TOF time resolution.

Figure 22 shows sensitivity of b, N_{part} and N_{coll} to variations of parameters (see descriptions in the figures) in the MC-Glauber of Au+Au collisions at $\sqrt{s_{NN}}$ = 7.7 GeV for centrality classes defined by track multiplicity in TPC. During sensitivity check primary particles were selected here using motherID cut. Parameters of the multiplicity fit functions for different N_a parametrizations are listed in the table 30:

Parametrization of N_a	f	μ	k	χ^2/ndf
$fN_{part} + (1-f)N_{coll}$	0.4	0.31	42	1.18
N_{coll}^{f}	0.99	0.28	91	1.34

Table 30: Parameters of the fit to the charged particle multiplicity for the different parametrizations of N_a.

Figure 23 shows track multiplicity in TPC for reconstructed Au+Au collisions at at $\sqrt{s_{NN}}$ = 7.7 GeV from UrQMD event generator for both methods.

Figure 24 shows centrality dependence of mean value of impact parameter $\langle b \rangle$ for reconstructed Au+Au collisions at at $\sqrt{s_{NN}}$ = 7.7 GeV from UrQMD event generator. Figure 24 (a) shows result for Glauber-based method, fig. 24 (b) shows result for Γ-fit.

Figure 25 shows centrality dependence of mean value of number of participants $\langle N_{part} \rangle$ and NN binary collisions $\langle N_{coll} \rangle$ for reconstructed Au+Au collisions at at $\sqrt{s_{NN}}$ = 7.7 GeV from UrQMD event generator. The description of fig. 25 (a), (b) is similar to fig. 24.

Table 31 show geometric properties (b, N_{part}, N_{coll}) of reconstructed Au+Au collisions at $\sqrt{s_{NN}}$ = 7.7 GeV from UrQMD event generator for centrality classes defined by sharp cuts in the track multiplicity distribution in TPC, simulated with an NBD-Glauber fit.

Centrality, %	N_{ch}^{min}	N_{ch}^{max}	$\langle b \rangle$, fm	RMS	b_{min}, fm	b_{max}, fm	$\langle N_{part} \rangle$	RMS	N_{part}^{min}	N_{part}^{max}	$\langle N_{coll} \rangle$	RMS	N_{coll}^{min}	N_{coll}^{max}
0 - 10	122	226	2.87	1.10	1.39	4.06	319.82	32.03	280.94	363.43	685.98	87.43	577.55	813.05
10 - 20	86	122	5.04	0.78	4.06	5.84	246.34	30.37	215.59	280.94	485.12	69.56	407.36	577.55
20 - 30	60	86	6.53	0.66	5.84	7.17	188.15	25.99	163.88	215.59	340.94	54.50	284.11	407.36
30 - 40	41	60	7.74	0.62	7.17	8.27	142.34	22.33	122.89	163.88	236.02	43.19	194.43	284.11
40 - 50	27	41	8.78	0.61	8.27	9.26	105.61	19.31	90.17	122.89	159.04	34.37	128.97	194.43
50 - 60	17	27	9.72	0.62	9.26	10.17	76.16	16.47	63.83	90.17	103.01	26.67	81.47	128.97
60 - 70	10	17	10.60	0.66	10.17	11.04	52.71	14.00	42.44	63.83	63.31	20.45	47.71	81.47
70 - 80	5	10	11.50	0.75	11.04	11.99	33.26	11.82	25.11	42.44	34.93	15.16	24.62	47.71
80 - 90	2	5	12.55	0.96	11.99	13.24	17.81	9.27	11.39	25.11	16.18	10.14	9.26	24.62

Table 31: Geometric properties (b, N_{part}, N_{coll}) of reconstructed Au+Au collisions at $\sqrt{s_{NN}}$=7.7 GeV from UrQMD model for centrality classes defined by sharp cuts in the charged particle multiplicity distribution, simulated with an NBD-Glauber fit. The mean values and the RMS are obtained with a Glauber Monte Carlo calculation.

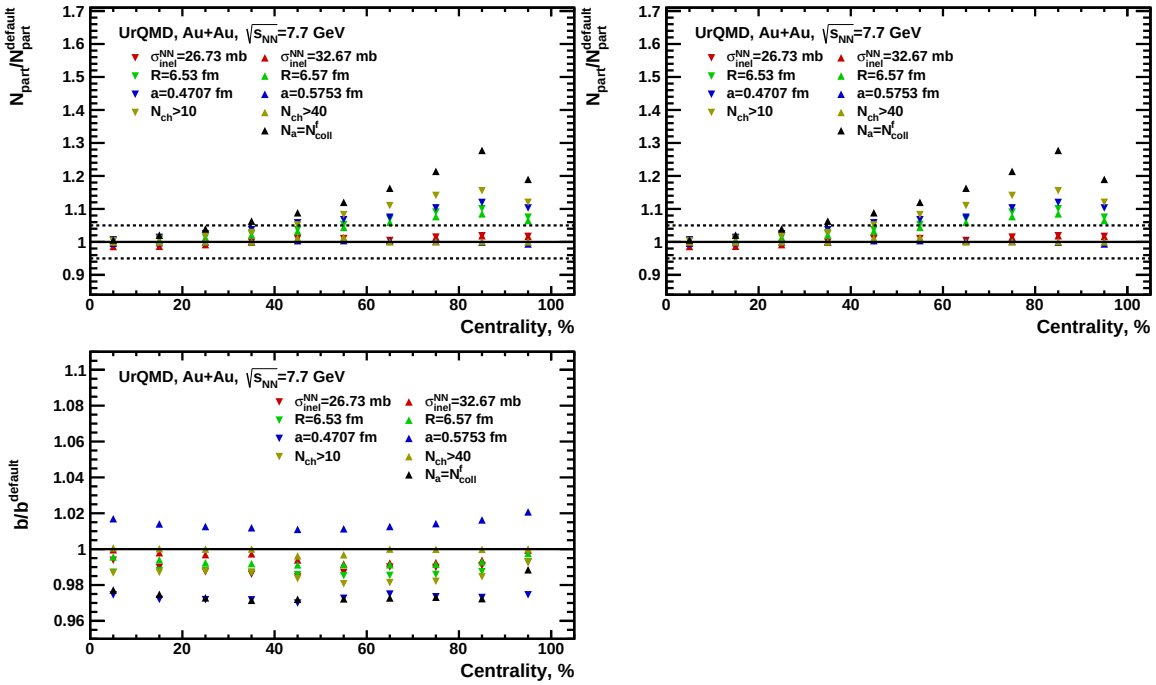

Figure 22: Sensitivity of b, N_{part} and N_{coll} to variations of parameters in the MC-Glauber of Au+Au collisions at $\sqrt{s_{NN}}$=7.7 GeV for centrality classes defined by track multiplicity in TPC. Primary particles were selected here using motherID cut.

Centrality, %	N_{ch}^{min}	N_{ch}^{max}	$\langle b \rangle$, fm	RMS	b_{min}, fm	b_{max}, fm
0 - 10	122	237	2.99	1.14	1.50	4.24
10 - 20	87	122	5.28	0.78	4.24	6.12
20 - 30	62	87	6.84	0.66	6.12	7.52
30 - 40	43	62	8.10	0.61	7.52	8.66
40 - 50	29	43	9.20	0.58	8.66	9.68
50 - 60	19	29	10.16	0.55	9.68	10.63
60 - 70	11	19	11.06	0.57	10.63	11.51
70 - 80	6	11	11.93	0.59	11.51	12.33
80 - 90	3	6	12.72	0.65	12.33	13.10
90 - 100	1	3	13.49	0.71	13.10	13.90

Table 32: The centrality clases, the mean value of impact parameter and the RMS from the reconstructed UrQMD events for Au+Au collisions at $\sqrt{s_{NN}}$ =7.7 GeV using Γ-fit approach.

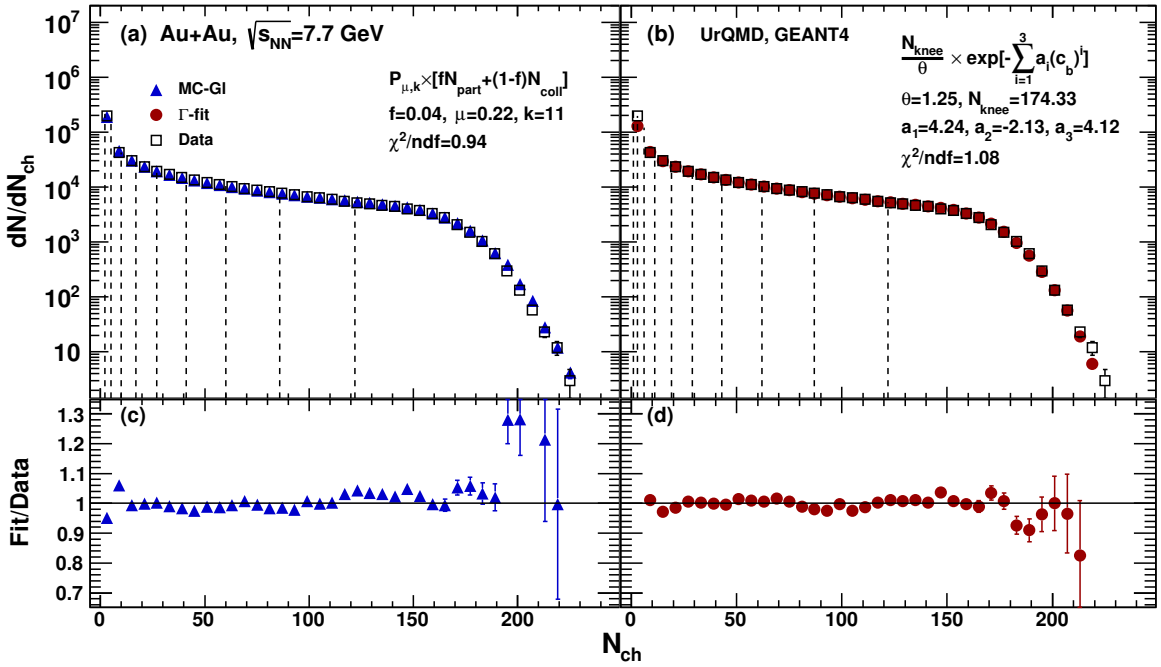

Figure 23: Distribution of the charged particle multiplicity reconstructed in TPC for Au+Au collisions at at $\sqrt{s_{NN}}$=7.7 GeV using UrQMD model as an event generator (open symbols). The distribution is fitted with the Glauber-based (blue triangles) and Γ-fit (red circles) fit functions. Vertical lines denote sharp cuts for centrality classes.

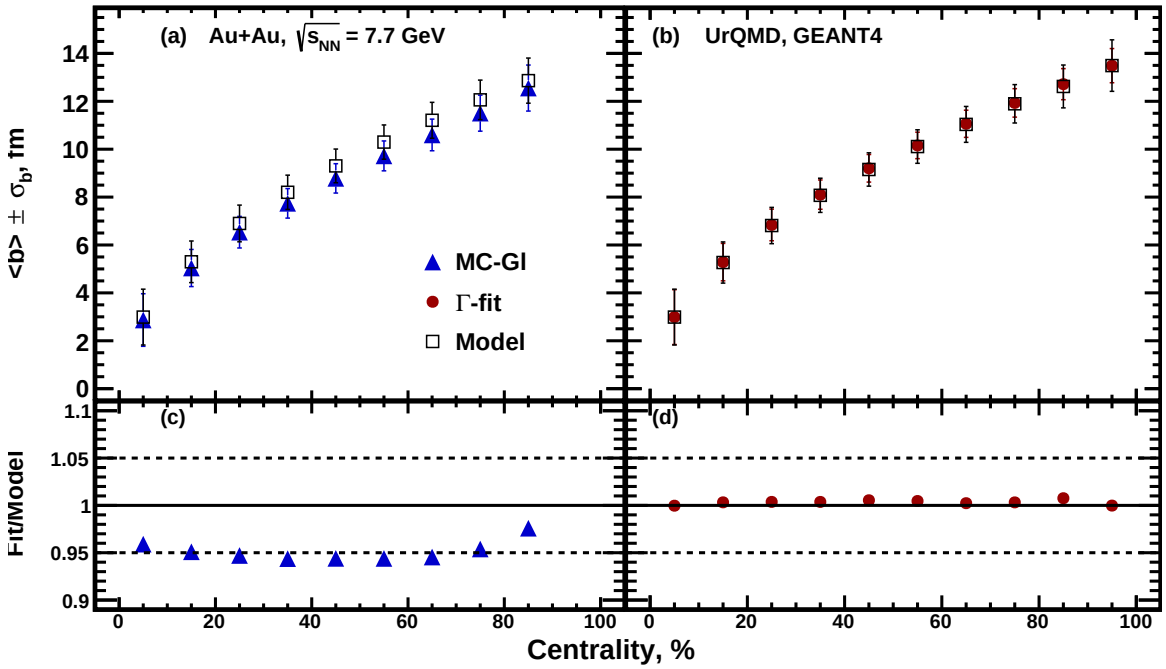

Figure 24: Centrality dependence of $\langle b \rangle$ for Au+Au collisions at at $\sqrt{s_{NN}}$=7.7 GeV from MC-Glauber (blue triangles), Γ-fit (red circles) calculations and UrQMD model (open symbols).

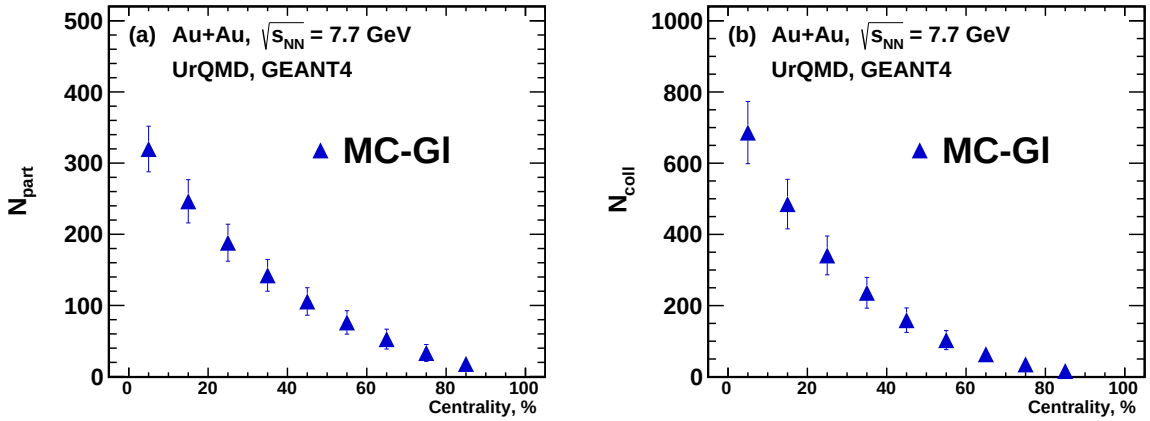

Figure 25: Centrality dependence of $\langle N_{part} \rangle$ (a) and $\langle N_{coll} \rangle$ (b) for Au+Au collisions at at $\sqrt{s_{NN}}$=7.7 GeV from MC-Glauber calculations (closed symbols) and UrQMD model (open symbols).

4.3 Reconstructed UrQMD Bi+Bi collisions at $\sqrt{s_{NN}}$=9.46 GeV

In this reconstructed data set, UrQMD model together with GEANT4 were used for Au+Au event generation at $\sqrt{s_{NN}}$ = 9.46 GeV and simulation of detector response in the MPD subsystems. Information provided from GEANT4 was reconstructed using dedicated reconstruction tools in MPDROOT framework. This data set was produced during the official production (Request 5 for PWG4) with modified particle decay configuration. This is a GEANT4 based general-purpose project, which includes simulation of the MPD-ECAL (ver.3 geometry) and has enhanced (x20) probabilities for light vector meson decays to ee+X channels. Since original branching for such decays is $10^{-4} - 10^{-5}$, the enhancement does not affect the simulation of hadrons. Decays of short-lived resonances (to have realistic peak widths) and pi0/eta-meson are managed by Pythia8.

Figure 26 shows sensitivity of b, N_{part} and N_{coll} to variations of parameters (see descriptions in the figures) in the MC-Glauber of Bi+Bi collisions at $\sqrt{s_{NN}}$ = 9.46 GeV for centrality classes defined by track multiplicity in TPC. During sensitivity check primary particles were selected here using motherID cut. Parameters of the multiplicity fit functions for different N_a parametrizations are listed in the table 33:

Parametrization of N_a	f	μ	k	χ^2/ndf
$fN_{part} + (1-f)N_{coll}$	0.34	0.22	41	0.99
N_{part}^{f}	1.22	0.11	1	1.02
N_{coll}^{f}	1.0	0.18	92	1.15
$\frac{(1-f)}{2}N_{part} + fN_{coll}$	0.67	0.24	50	0.97

Table 33: Parameters of the fit to the charged particle multiplicity for the different parametrizations of N_a.

Figure 27 shows track multiplicity in TPC for reconstructed Bi+Bi collisions at $\sqrt{s_{NN}} = 9.46$ GeV from UrQMD event generator for both methods.

Figure 28 shows centrality dependence of mean value of impact parameter $\langle b \rangle$ for reconstructed Bi+Bi collisions at $\sqrt{s_{NN}} = 9.46$ GeV from UrQMD event generator. Figure 28 (a) shows result for Glauber-based method, fig. 28 (b) shows result for Γ-fit.

Figure 29 shows centrality dependence of mean value of number of participants $\langle N_{part} \rangle$ and NN binary collisions $\langle N_{coll} \rangle$ for reconstructed Bi+Bi collisions at $\sqrt{s_{NN}} = 9.46$ GeV from UrQMD event generator. The description of fig. 29 (a), (b) is similar to fig. 28.

Table 34 shows geometric properties (b, N_{part}, N_{coll}) of reconstructed Bi+Bi collisions at $\sqrt{s_{NN}}$ = 9.46 GeV from UrQMD event generator for centrality classes defined by sharp cuts in the track multiplicity distribution in TPC, simulated with an NBD-Glauber fit. Table 35 shows geometric properties for Γ-fit.

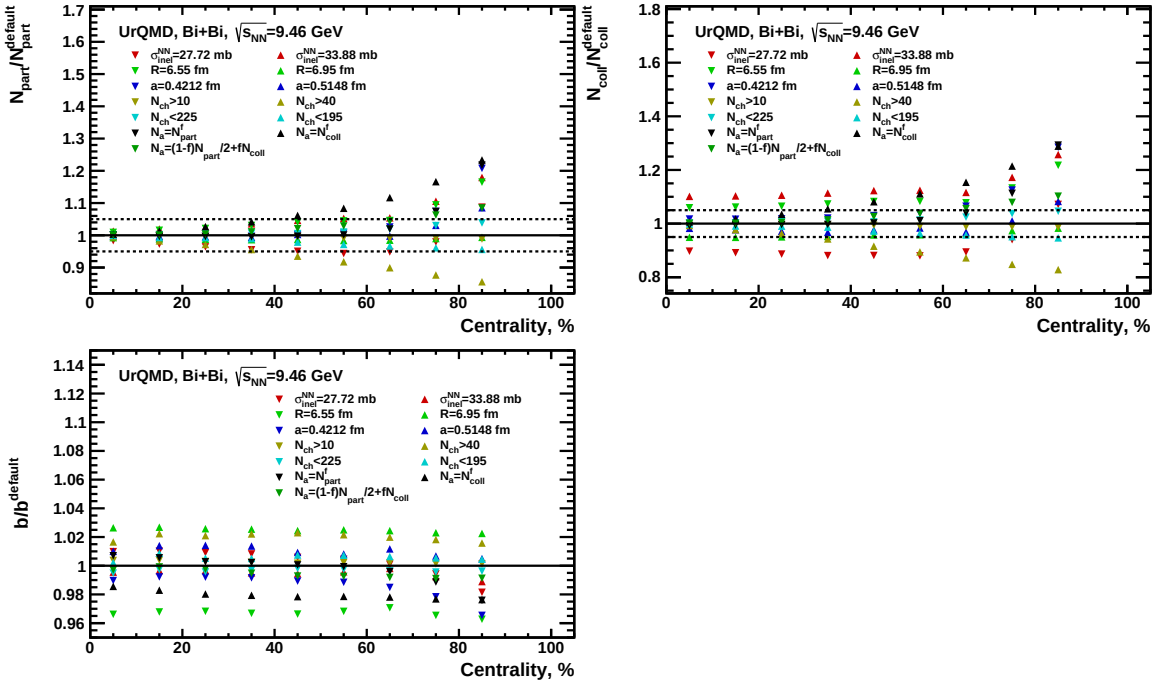

Figure 26: Sensitivity of b, N_{part} and N_{coll} to variations of parameters in the MC-Glauber of Bi+Bi collisions at $\sqrt{s_{NN}}$=9.46 GeV for centrality classes defined by charged particle multiplicity in TPC. Primary particles were selected here using motherID cut.

Centrality, %	N_{ch}^{min}	N_{ch}^{max}	$\langle b \rangle$, fm	RMS	b_{min}, fm	b_{max}, fm	$\langle N_{part} \rangle$	RMS	N_{part}^{min}	N_{part}^{max}	$\langle N_{coll} \rangle$	RMS	N_{coll}^{min}	N_{coll}^{max}
0 - 10	141	260	2.89	1.10	1.26	4.14	342.35	34.05	299.04	393.74	777.46	96.90	652.69	927.25
10 - 20	99	141	5.12	0.76	4.14	5.95	262.24	31.55	228.83	299.04	548.21	75.87	459.75	652.69
20 - 30	69	99	6.65	0.64	5.95	7.28	199.82	26.68	174.37	228.83	385.22	58.86	321.34	459.75
30 - 40	47	69	7.88	0.60	7.28	8.41	150.87	22.89	130.60	174.37	266.38	46.60	219.86	321.34
40 - 50	31	47	8.94	0.59	8.41	9.44	111.93	19.52	95.01	130.60	179.49	36.51	144.79	219.86
50 - 60	19	31	9.90	0.60	9.44	10.37	80.32	16.78	66.60	95.01	115.43	28.62	90.34	144.79
60 - 70	11	19	10.80	0.63	10.37	11.20	54.93	13.98	44.83	66.60	69.70	21.46	53.06	90.34
70 - 80	6	11	11.63	0.69	11.20	12.01	35.82	11.60	28.53	44.83	39.80	15.74	29.50	53.06
80 - 90	3	6	12.45	0.80	12.01	13.09	21.79	9.45	14.86	28.53	21.21	11.21	13.79	29.50
90 - 100	1	2	13.91	1.07	13.09	15.00	7.39	5.61	-1.77	14.86	5.82	5.39	-4.67	13.79

Table 34: Geometric properties (b, N_{part}, N_{coll}) of reconstructed Bi+Bi collisions at $\sqrt{s_{NN}}$=9.46 GeV from UrQMD model for centrality classes defined by sharp cuts in the charged particle multiplicity distribution, simulated with an NBD-Glauber fit. The mean values and the RMS are obtained with a Glauber Monte Carlo calculation.

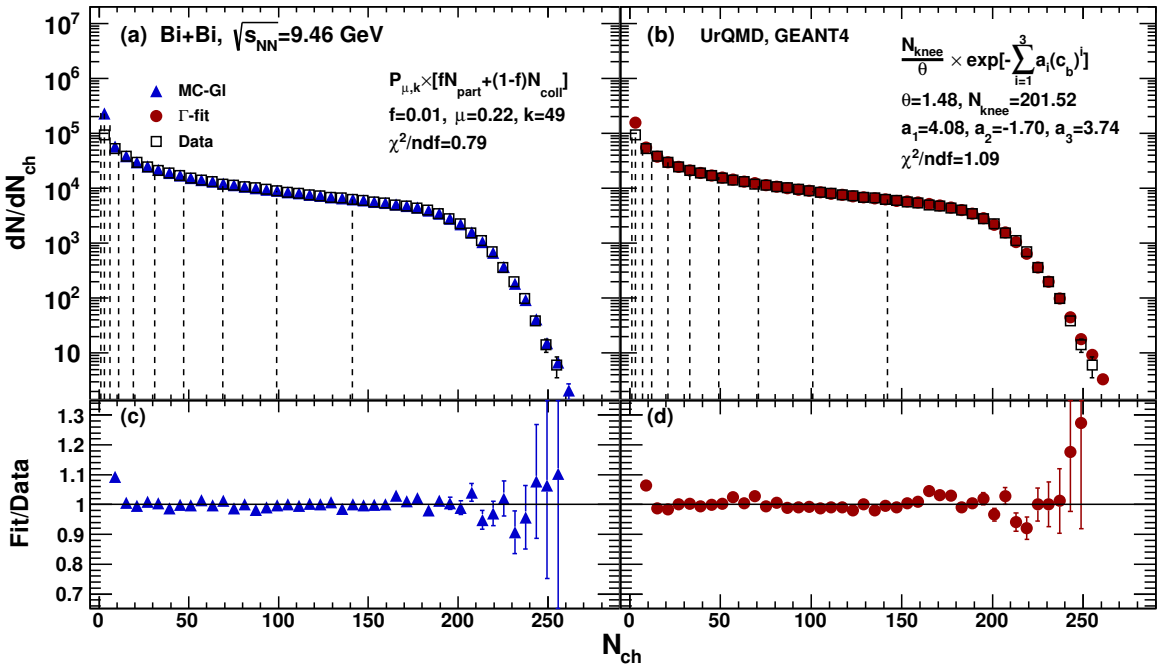

Figure 27: Distribution of the charged particle multiplicity reconstructed in TPC for Bi+Bi collisions at at $\sqrt{s_{NN}}$=9.46 GeV using UrQMD model as an event generator (open symbols). The distribution is fitted with the Glauber-based (blue triangles) and Γ-fit (red circles) fit functions. Vertical lines denote sharp cuts for centrality classes.

Centrality, %	N_{ch}^{min}	N_{ch}^{max}	$\langle b\rangle$, fm	RMS	b_{min}, fm	b_{max}, fm
0 - 10	142	284	3.03	1.16	1.49	4.30
10 - 20	101	142	5.37	0.80	4.30	6.23
20 - 30	71	101	6.97	0.68	6.23	7.66
30 - 40	49	71	8.27	0.62	7.66	8.82
40 - 50	33	49	9.36	0.58	8.82	9.86
50 - 60	21	33	10.34	0.57	9.86	10.82
60 - 70	12	21	11.27	0.58	10.82	11.70
70 - 80	7	12	12.10	0.60	11.70	12.52
80 - 90	3	7	12.92	0.69	12.52	13.32
90 - 100	1	3	13.74	0.73	13.32	14.23

Table 35: The centrality clases, the mean value of impact parameter and the RMS from the reconstructed UrQMD events for Bi+Bi collisions at $\sqrt{s_{NN}}$ =9.46 GeV using Γ-fit approach.

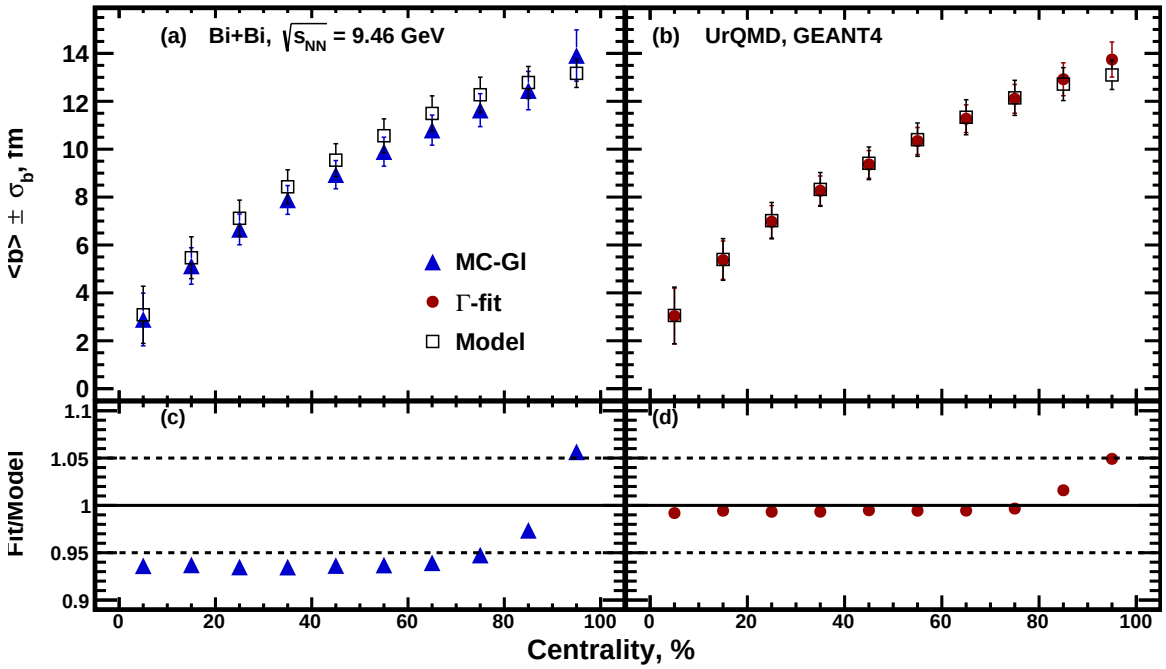

Figure 28: Centrality dependence of $\langle b \rangle$ for Bi+Bi collisions at at $\sqrt{s_{NN}}$=9.46 GeV from MC-Glauber (blue triangles), Γ-fit (red circles) calculations and UrQMD model (open symbols).

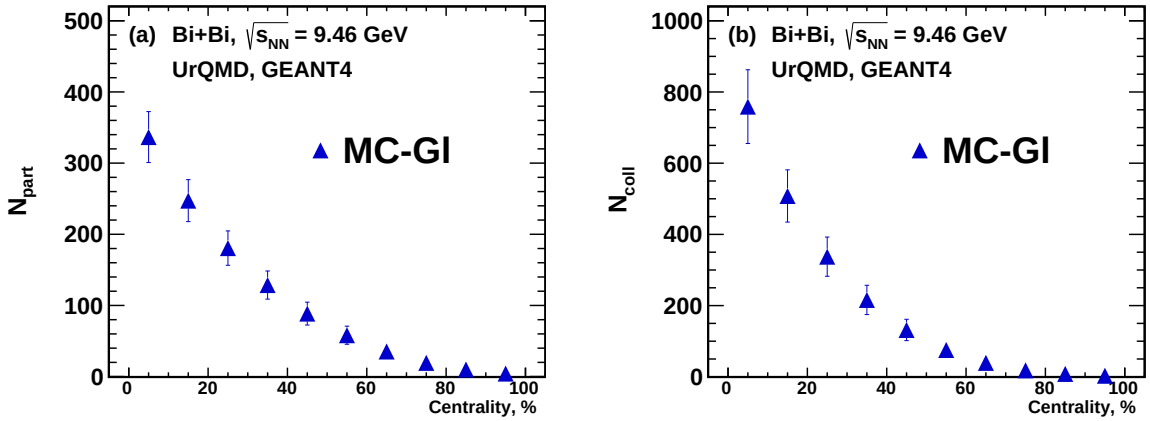

Figure 29: Centrality dependence of $\langle N_{part} \rangle$ (a) and $\langle N_{coll} \rangle$ (b) for Bi+Bi collisions at at $\sqrt{s_{NN}}$=9.46 GeV from MC-Glauber calculations (closed symbols) and UrQMD model (open symbols).

4.4 Reconstructed PHQMD Au+Au collisions at $\sqrt{s_{NN}}$=9 GeV

In this reconstructed data set, PHQMD model together with GEANT3 were used for Au+Au event generation at $\sqrt{s_{NN}} = 9$ GeV and simulation of detector response in the MPD subsystems. Information provided from GEANT3 was reconstructed using dedicated reconstruction tools in MPDROOT framework. This data set was produced during the official production (Request 7 PWG2) with the recent modifications in the dE/dx simulation and tracking. The data set produced for a variety of feasibility studies, such as hadron spectra and yields, multi-strangeness production, light nuclei production, and hypernuclei reconstruction.

Figure 30 shows sensitivity of b, N_{part} and N_{coll} to variations of parameters (see descriptions in the figures) in the MC-Glauber of Au+Au collisions at $\sqrt{s_{NN}} = 9$ GeV for centrality classes defined by track multiplicity in TPC. During sensitivity check primary particles were selected here using motherID cut. Parameters of the multiplicity fit functions for different N_a parametrizations are listed in the table 36:

Parametrization of N_a	f	μ	k	χ^2/ndf
$fN_{part} + (1-f)N_{coll}$	0.04	0.25	7	1.59
N_{part}^{f}	1.38	0.06	37	1.71
N_{coll}^{f}	1.0	0.24	24	1.73
$\frac{(1-f)}{2}N_{part} + fN_{coll}$	0.88	0.27	3	1.62

Table 36: Parameters of the fit to the charged particle multiplicity for the different parametrizations of N_a.

Figure 31 shows track multiplicity in TPC for reconstructed Bi+Bi collisions at $\sqrt{s_{NN}} = 9$ GeV from PHQMD event generator for both methods.

Figure 32 shows centrality dependence of mean value of impact parameter $\langle b \rangle$ for reconstructed Bi+Bi collisions at $\sqrt{s_{NN}} = 9$ GeV from PHQMD event generator. Figure 32 (a) shows result for Glauber-based method, fig. 32 (b) shows result for Γ-fit.

Figure 33 shows centrality dependence of mean value of number of participants $\langle N_{part} \rangle$ and NN binary collisions $\langle N_{coll} \rangle$ for reconstructed Bi+Bi collisions at $\sqrt{s_{NN}} = 9$ GeV from PHQMD event generator. The description of fig. 33 (a), (b) is similar to fig. 32.

Table 37 shows geometric properties (b, N_{part}, N_{coll}) of reconstructed Bi+Bi collisions at $\sqrt{s_{NN}}$ = 9 GeV from PHQMD event generator for centrality classes defined by sharp cuts in the track multiplicity distribution in TPC, simulated with an NBD-Glauber fit. Table 38 shows geometric properties for Γ-fit.

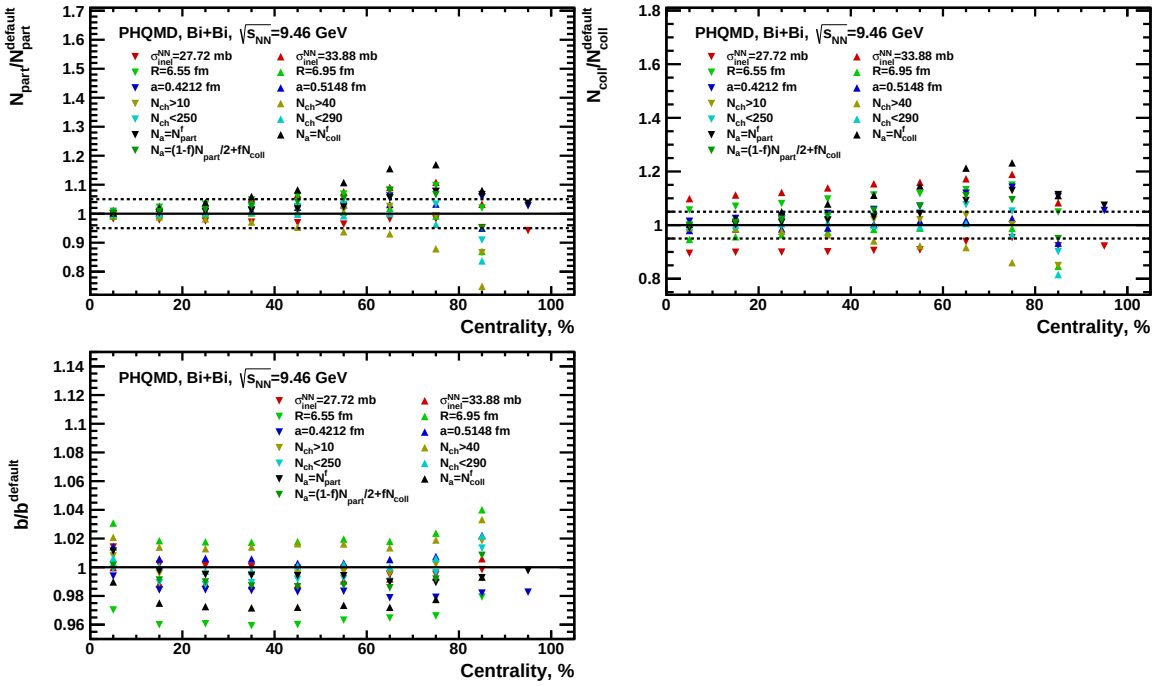

Figure 30: Sensitivity of b, N_{part} and N_{coll} to variations of parameters in the MC-Glauber of Bi+Bi collisions at $\sqrt{s_{NN}}$=9 GeV for centrality classes defined by charged particle multiplicity in TPC. Primary particles were selected here using motherID cut.

Centrality, %	N_{ch}^{min}	N_{ch}^{max}	$\langle b \rangle$, fm	RMS	b_{min}, fm	b_{max}, fm	$\langle N_{part} \rangle$	RMS	N_{part}^{min}	N_{part}^{max}	$\langle N_{coll} \rangle$	RMS	N_{coll}^{min}	N_{coll}^{max}
0 - 10	118	220	2.89	1.12	1.38	4.08	342.31	34.60	301.01	389.76	777.42	98.63	657.41	919.20
10 - 20	84	118	5.06	0.80	4.08	5.87	264.73	32.83	232.37	301.01	555.19	79.99	468.73	657.41
20 - 30	59	84	6.56	0.68	5.87	7.21	203.47	28.43	177.47	232.37	394.46	63.99	329.51	468.73
30 - 40	40	59	7.80	0.65	7.21	8.36	153.88	24.79	132.65	177.47	273.67	51.77	225.03	329.51
40 - 50	26	40	8.90	0.64	8.36	9.41	113.33	21.36	96.05	132.65	182.58	40.94	146.91	225.03
50 - 60	16	26	9.89	0.65	9.41	10.36	80.80	18.22	66.86	96.05	116.55	31.75	90.59	146.91
60 - 70	9	16	10.82	0.68	10.36	11.24	54.64	15.44	44.40	66.86	69.48	24.08	52.73	90.59
70 - 80	5	9	11.66	0.74	11.24	12.11	35.41	12.60	27.37	44.40	39.41	17.27	28.69	52.73
80 - 90	2	5	12.61	0.92	12.11	13.21	20.09	10.46	12.96	27.37	19.41	12.33	9.94	28.69

Table 37: Geometric properties (b, N_{part}, N_{coll}) of reconstructed Bi+Bi collisions at $\sqrt{s_{NN}}$=9 GeV from PHQMD model for centrality classes defined by sharp cuts in the charged particle multiplicity distribution, simulated with an NBD-Glauber fit. The mean values and the RMS are obtained with a Glauber Monte Carlo calculation.

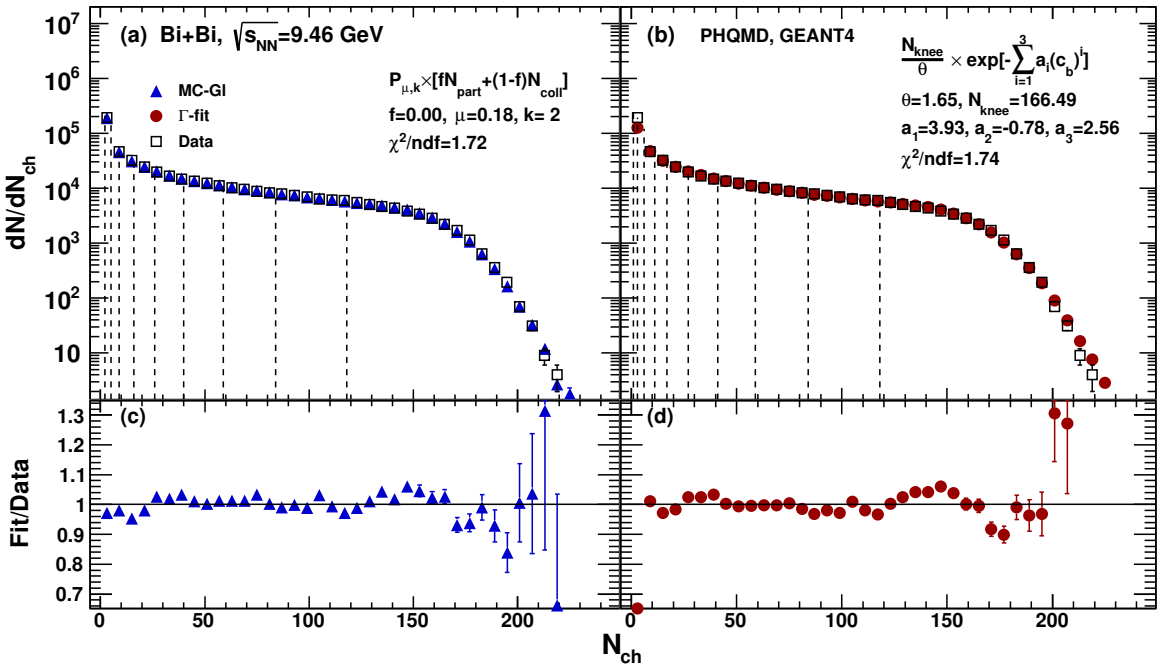

Figure 31: Distribution of the charged particle multiplicity reconstructed in TPC for Bi+Bi collisions at at $\sqrt{s_{NN}}$=9 GeV using PHQMD model as an event generator (open symbols). The distribution is fitted with the Glauber-based (blue triangles) and Γ-fit (red circles) fit functions. Vertical lines denote sharp cuts for centrality classes.

Centrality, %	N_{ch}^{min}	N_{ch}^{max}	$\langle b \rangle$, fm	RMS	b_{min}, fm	b_{max}, fm
0 - 10	118	236	3.07	1.20	1.58	4.31
10 - 20	84	118	5.35	0.87	4.31	6.20
20 - 30	59	84	6.94	0.73	6.20	7.62
30 - 40	41	59	8.22	0.67	7.62	8.80
40 - 50	27	41	9.33	0.66	8.80	9.84
50 - 60	17	27	10.36	0.66	9.84	10.80
60 - 70	11	17	11.23	0.66	10.80	11.68
70 - 80	6	11	12.07	0.74	11.68	12.49
80 - 90	3	6	12.91	0.80	12.49	13.29
90 - 100	1	3	13.73	0.85	13.29	14.24

Table 38: The centrality clases, the mean value of impact parameter and the RMS from the reconstructed PHQMD events for Bi+Bi collisions at $\sqrt{s_{NN}}$ =9 GeV using Γ-fit approach.

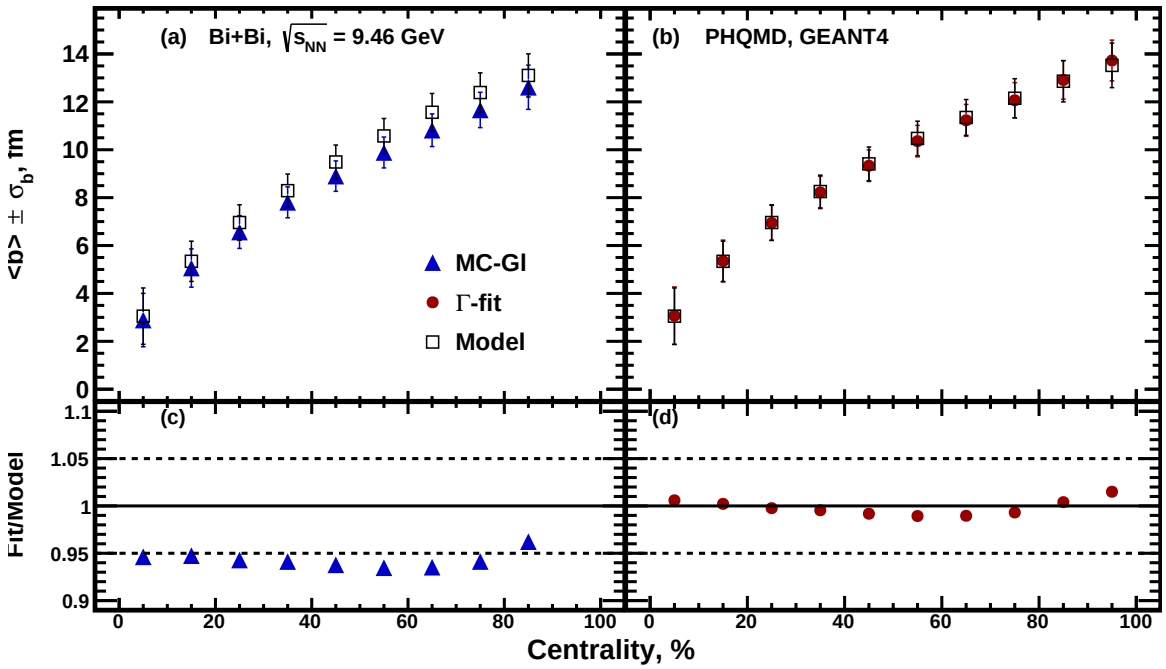

Figure 32: Centrality dependence of $\langle b \rangle$ for Bi+Bi collisions at at $\sqrt{s_{NN}}$=9 GeV from MC-Glauber (blue triangles), Γ-fit (red circles) calculations and PHQMD model (open symbols).

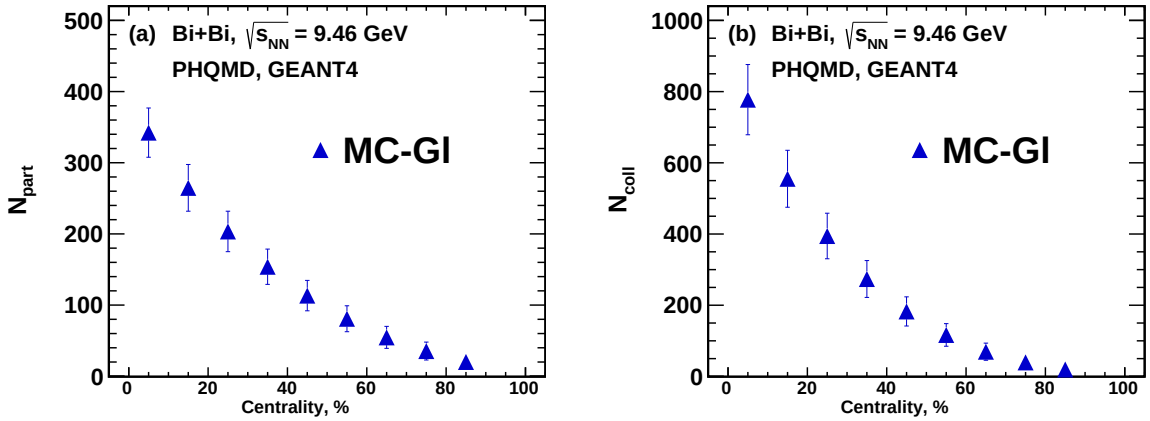

Figure 33: Centrality dependence of $\langle N_{part} \rangle$ (a) and $\langle N_{coll} \rangle$ (b) for Bi+Bi collisions at at $\sqrt{s_{NN}}$=9 GeV from MC-Glauber calculations (closed symbols) and PHQMD model (open symbols).

Acknowledgements

The authors thank Ilya Selyuzhenkov for helpful discussions and comments and Ilya Segal for helping with the Glauber-based centrality framework interface. Computational resources were provided by the NRNU MEPhI high-performance computing center and NICA high-performance cluster of LHEP JINR.

This research was funded by the RFBR according to the research project No. 18-02-40086 and partially supported by the European Union's Horizon 2020 research and innovation program under grant agreement No. 871072 and by the Ministry of Science and Higher Education of the Russian Federation, Project "Fundamental properties of elementary particles and cosmology" No. 0723-2020-0041.

References

[1] B. Abelev *et al.*, *Phys. Rev. C*, vol. 88, no. 4, p. 044 909, 2013.

[2] E. Zherebtsova, V. Klochkov, I. Selyuzhenkov, *et al.*, *EPJ Web Conf.*, vol. 182, p. 02 132, 2018.

[3] L. Adamczyk *et al.*, *Phys. Rev. C*, vol. 86, p. 054 908, 2012.

[4] V. Klochkov and I. Selyuzhenkov, *Acta Phys. Polon. Supp.*, vol. 10, p. 919, 2017.

[5] D. Kharzeev and M. Nardi, *Phys. Lett. B*, vol. 507, pp. 121–128, 2001.

[6] C. Loizides, J. Nagle, and P. Steinberg, *SoftwareX*, vol. 1-2, pp. 13–18, 2015.

[7] C. De Jager, H. De Vries, and C. De Vries, *Atomic Data and Nuclear Data Tables*, vol. 14, no. 5, pp. 479–508, 1974, Nuclear Charge and Moment Distributions.

[8] H. De Vries, C. W. De Jager, and C. De Vries, *Atom. Data Nucl. Data Tabl.*, vol. 36, pp. 495–536, 1987.

[9] S. Eidelman, K. Hayes, K. Olive, *et al.*, *Physics Letters B*, vol. 592, no. 1, pp. 1–5, 2004, Review of Particle Physics.

[10] P. D. Group, P. A. Zyla, R. M. Barnett, *et al.*, *Progress of Theoretical and Experimental Physics*, vol. 2020, no. 8, 2020, 083C01.

[11] R. Rogly, G. Giacalone, and J.-Y. Ollitrault, *Phys. Rev. C*, vol. 98, no. 2, p. 024 902, 2018.

[12] S. J. Das, G. Giacalone, P.-A. Monard, and J.-Y. Ollitrault, *Phys. Rev. C*, vol. 97, no. 1, p. 014 905, 2018.

[13] S. A. Bass *et al.*, *Prog. Part. Nucl. Phys.*, vol. 41, pp. 255–369, 1998.

[14] Z.-W. Lin, C. M. Ko, B.-A. Li, *et al.*, *Phys. Rev. C*, vol. 72, p. 064 901, 2005.

[15] V. Toneev and K. Gudima, *Nuclear Physics A*, vol. 400, pp. 173–189, 1983.

[16] A. S. Botvina, K. K. Gudima, J. Steinheimer, *et al.*, *Phys. Rev. C*, vol. 84, p. 064 904, 6 2011.

[17] J. Aichelin, E. Bratkovskaya, A. Le Fèvre, *et al.*, *Phys. Rev. C*, vol. 101, no. 4, p. 044 905, 2020.